9950 - 524

daedalus ENTERPRISES INC.
P.O. Box 1869, Ann Arbor, Michigan 48106 USA, (313) 769-5649
Cable Daedalus Telex 230531

Report Number 78004-01

DESIGN STUDY FOR THERMAL INFRARED MULTISPECTRAL SCANNER (TIMS)

FINAL REPORT
JPL CONTRACT #955829

C. G. Stanich
F. G. Osterwisch
D. M. Szeles, *Consultant*
W. H. Houtman, *Consultant*

Submitted by:

DAEDALUS ENTERPRISES, INC.
Ann Arbor, Michigan

Submitted to:

JET PROPULSION LABORATORY
California Institute of Technology
Pasadena, California

MARCH 27, 1981

This work was performed for the Jet Propulsion Laboratory, California Institute of Technology sponsored by the National Aeronautics and Space Administration under Contract NAS7-100

This document contains information prepared by DAEDALUS ENTERPRISES, INC. under JPL sub-contract. Its content is not necessarily endorsed by the Jet Propulsion Laboratory, California Institute of Technology, or its sponsors.

TABLE OF CONTENTS

LIST OF ILLUSTRATIONS

LIST OF TABLES

ABSTRACT

Study contract 955829 was awarded to ascertain the feasibility of dividing the 8-12 μm thermal infrared wavelength region into six spectral bands by an airborne line scanner system; and if feasibility were determined, to design such a system for remote sensing of the earth's surface. The desired performance was to be achieved by combining the optical system of an existing scanner design with a 6-band spectrometer of new design, with emphasis placed on using proven technology to produce a practical instrument. The report presents the results of this hardware design and analyzes the expected performance of such a system.

The study concentrated on the main elements of the spectrometer design; its components being the collimator, the dispersing element, the focusing optic, the sensor array, and the mechanical assembly required to hold these elements while maintaining their alignment throughout the operating temperature range. The modifications required to an existing scanner design were also examined.

Contract NAS13-170 has been awarded by NASA/NSTL to construct a system based on this design study. Completion of the system is planned for April, 1982.

SUMMARY

This report verifies the feasibility of constructing an airborne multispectral scanner system, operating in six spectral bands between 8.2 and 12.2 μm, and presents a design for such an instrument. The feasibility is verified by analyzing radiometric sensitivity performance, optical component performance, and mechanical component performance. These three analyses confirm 1) that the necessary optical components can be built to the required tolerances; 2) that the mechanical assembly as designed can maintain the required alignment of the optical components; and 3) that the radiometric sensitivity of the instrument will surpass a design goal of NETD $\leq$ 0.3°C in each spectral band.

The design presented uses the optical system design of an existing scanner system and a 6-band spectrometer designed under this contract. Elements specified in the spectrometer design include an off-axis reflective collimator, a reflective diffraction grating, a triplet germanium imaging lens, a photoconductive mercury-cadmium-telluride sensor array, and the mechanical assembly to hold these parts and maintain their optical alignment across a broad temperature range. The existing scanner design is modified to accept the new spectrometer and two field-filling thermal reference sources.

1
INTRODUCTION

The thermal infrared multispectral scanner includes two optical assemblies of major importance to this study: the primary collecting telescope and the secondary spectrometer. These two assemblies are connected optically through an aperture or field stop which defines the instantaneous field of view of the system. The function of the primary telescope is to collect incoming radiation and focus it onto the aperture. The spectrometer disperses this radiation spectrally and reimages it onto an array of detectors. The detector array converts the radiation into an electrical signal for processing and recording. The complete system is mounted in an aircraft such that the primary telescope may receive radiation from the earth through an opening in the aircraft. A 45° rotating scan mirror traverses the primary field of view at a right angle to the aircraft flight direction. Forward motion of the aircraft ensures that during each rotation the scan mirror receives radiation from a new area of the ground scene beneath the aircraft.

Figure 1 shows the optical layout of the complete system. The rotating scan mirror (not shown) directs energy from the ground onto the primary focusing parabolic mirror (M1). Deviating mirror (M2) deflects the converging rays of energy out of the primary field of view and up to the field stop. Energy passing through the field stop is collimated by mirror (M3), an off-axis paraboloid section. Mirror (M3) directs the collimated radiation onto the diffraction grating (M4) which reflects and disperses it spectrally. Lens (L1) focuses the energy from the diffraction grating through an optical bandpass filter and onto a linear array of detector elements. The optical filter passes only radiation within the 8.2-12.2 μm wavelengths of interest.

Each detector element is positioned in the image plane to intercept energy within specific wavelength boundaries. Each

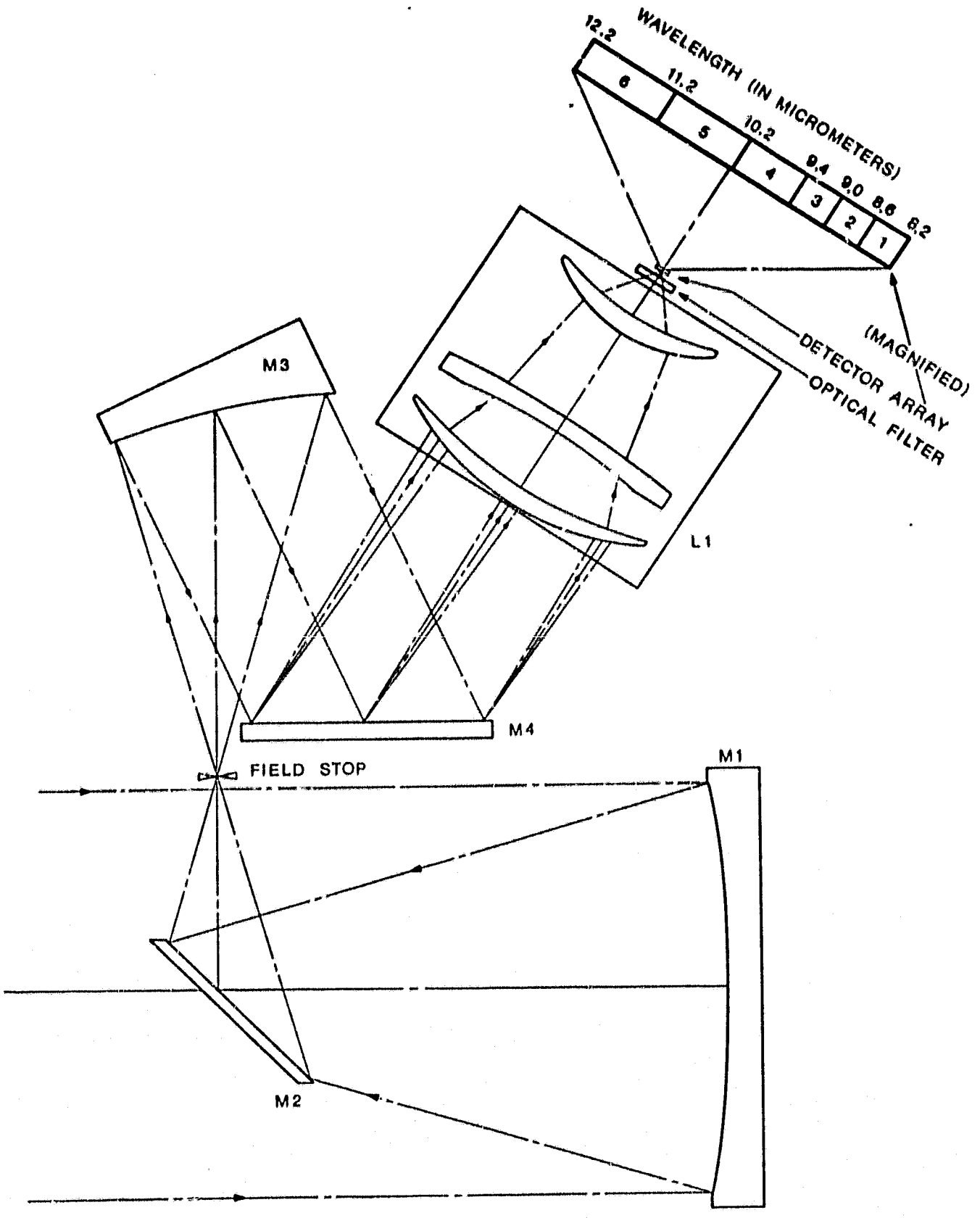

FIGURE 1
TIMS OPTICAL LAYOUT

detector converts its incident energy into an electrical signal which is then amplified and processed by the system electronics. The optical filter and the detector array are contained within a vacuum dewar and cooled to 77°K by liquid nitrogen.

Significant parameters of the TIMS primary telescope and spectrometer are given below.

Primary Optics	axial paraboloid 13" effective focal length 7.5" clear aperture 36 sq. inch active area
Ground Resolution	2.5 milliradians
Maximum Scan Rate	25 revolutions per second
Noise Bandwidth	32 KHz
Spectrometer	collimator dispersive element focusing optic detector array
Spectral Bands	(6) from 8.2 to 12.2 μm 8.2 to 8.6 μm bandwidth 0.4 μm 8.6 to 9.0 μm bandwidth 0.4 μm 9.0 to 9.4 μm bandwidth 0.4 μm 9.4 to 10.2 μm bandwidth 0.8 μm 10.2 to 11.2 μm bandwidth 1.0 μm 11.2 to 12.2 μm bandwidth 1.0 μm
Sensitivity	0.3°C maximum
Operating Temperature	-55°C to +50°C

2
TECHNICAL DISCUSSION

2.1. PRIMARY TELESCOPE

The primary telescope encompasses the optical components that collect the energy from the ground scene and reimages it onto the field stop. When the mechanics of mirror rotation and reference sources are included, it is commonly referred to as a "scan head". The primary telescope is a classic Newtonian design with a field of view which is traversed by a scan mirror. The scan mirror is a flat, single facet optical mirror oriented at 45° and centered with respect to its axis of rotation. The mirror is mounted directly on the shaft of a DC motor along with an optical shaft encoder. A 13" focal length focusing paraboloid, a 3" diameter secondary mirror, and a field stop aperture are thermally compensated to remain in focus throughout the entire operating temperature range of the scan head.

The scan head contains focusing optics, an electro-optical scanning assembly, two controlled thermal reference sources, and provisions for mounting the thermal spectrometer. These elements are mounted onto an aluminum and steel structure which is designed to mechanically support the individual assemblies and also to maintain the optical performance over a wide temperature range. The scan head includes covers to shield against stray radiation, to protect the optics during flight, and to minimize thermal gradients across the scan head.

A cross-sectional view of the scan head is shown in Figure 2. The rotating mirror directs the energy received from the ground scene onto the 13" focal length paraboloidal primary focusing mirror. The energy is then reflected by a flat secondary mirror where the field of view determining aperture is located in the focal plane just above the clear aperture of the primary mirror.

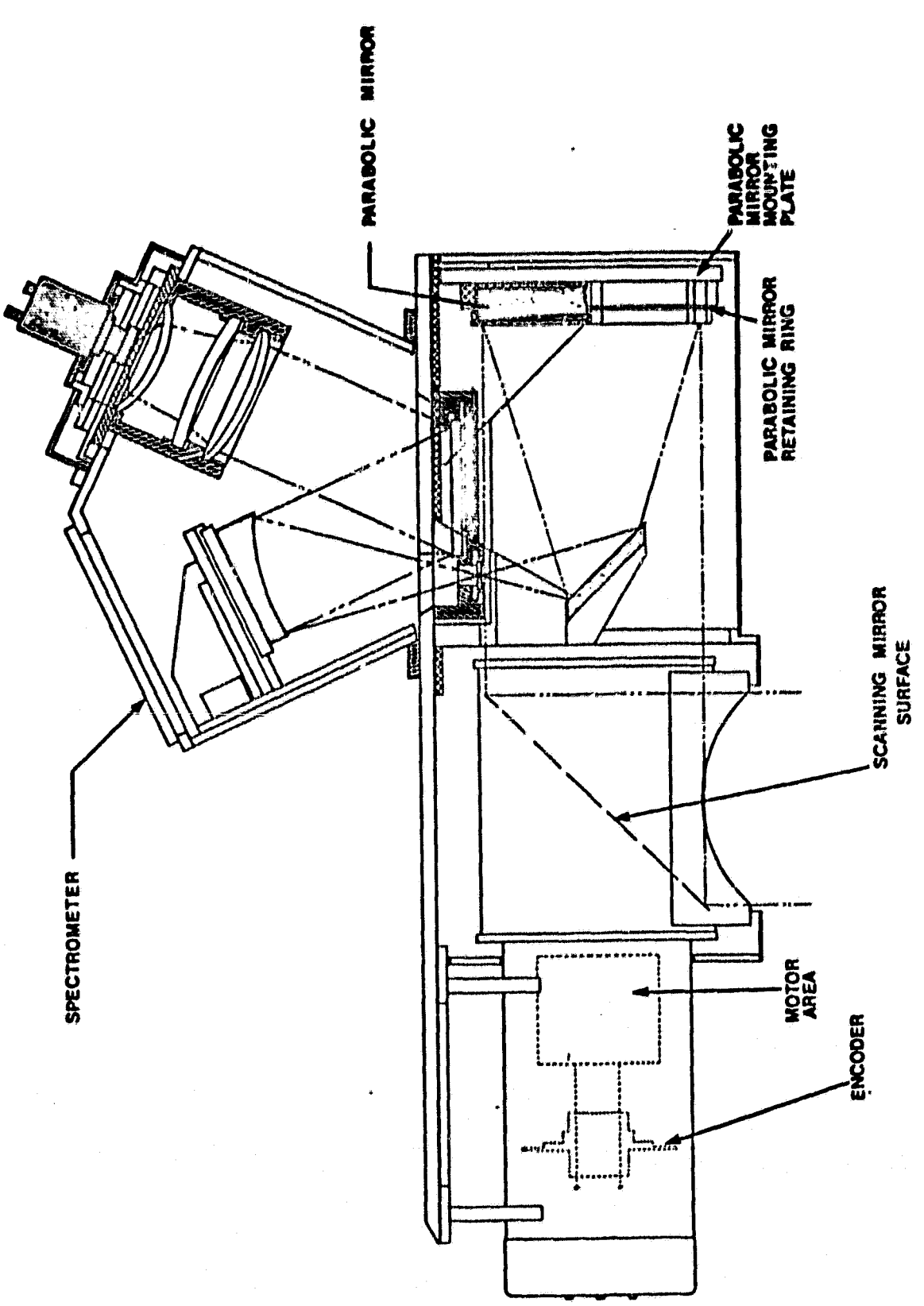

FIGURE 2. TIMS SCAN HEAD CROSS SECTION

2.1.1. THERMAL COMPENSATION

The design of the scan head takes into account the differing coefficients of thermal expansion of the various materials used in its construction. The basic structure of the scan head is an aluminum "U" shaped channel. The motor/mirror/encoder is housed in stainless steel and positioned on the aluminum channel with four stainless steel pins. Three of the pins fit into slotted holes in the motor assembly, while the fourth pin is press fitted into the assembly on the aluminum channel. Eight bolts are used to secure the assembly to the scan head channel. The slotted alignment pins allow the steel motor case to expand and contract at a different rate than the aluminum structure while maintaining the assembly's critical alignment with respect to the telescope optics.

The primary focusing mirror is mounted in a plate and ring assembly manufactured of Invar steel. The special glass substrate used in the primary mirror has a temperature coefficient of expansion that is very low and closely matches that of the Invar steel. This low expansion material produces a mirror with an optical variation as a function of temperature which is small enough to be ignored in the thermal compensation scheme. The Invar steel mirror mount is then attached to an aluminum plate with a series of threaded fasteners passing through Belleville compression washers and oversized holes in the mounting plate. The optical alignment and thermal compensation is achieved with the use of two stainless steel pins. The pins are attached to the aluminum plate and fitted into the alignment holes in the mirror mount. One hole in the mirror mount is press fit, while the other is slotted in the direction of the vertical axis of the scanner. This allows movement to occur, as the mirror mount and plate have markedly different coefficients of expansion.

The flat secondary mirror is glued to an aluminum mount which protrudes into the optical path from the top of the

scan head. This secondary mirror mount is fastened to a "sled"; so called because it is an assembly which slides in a carefully designed fashion with respect to the channel. The method to accomplish this controlled sliding is to constrain the sled movement with two long Invar steel bars. One end of each bar is pinned to the sled, and the other ends are pinned to the aluminum channel. A similar arrangement is used to mount the spectrometer onto the sled. Two short Invar steel bars are used to constrain the movement of the spectrometer in a controlled manner. One end of each of these bars is pinned to the spectrometer, while the other ends are pinned to the sled. The sled and the spectrometer have flat keys and keyways which restrict their movement to a direction parallel to the optical axis of the scanner. The spectrometer, sled and four Invar bars are attached with threaded fasteners using Belleville compression washers. Mounting holes are oversized and mating surfaces are Teflon® coated to reduce friction and permit (controlled) sliding movement.

This rather complex mechanical assembly maintains the spectrometer aperture precisely in the focal plane and centered about the principal axis of the primary telescope over a broad temperature range. The expansion and contraction of the secondary mirror mount, primary mirror mount, and scan head channel are compensated by the movement of the primary mirror, secondary mirror and spectrometer aperture.

2.1.2. SCAN HEAD MODIFICATION

The original design of the scan head used a high resolution five band spectrometer in the secondary optics of the system, operating in the visible/near infrared portion of the spectrum. Although the optical design is unaltered, some modification of the scan head structure was necessary to permit its use in the TIMS system. Two new constraints on the design are: 1) the addition of two calibrated thermal reference sources (blackbodies); and 2) a more complex and physically larger spectrometer to be interfaced to the primary telescope.

The addition of the thermal reference sources to the scan head considers the following criteria:

1. They will each completely fill the field of view of the primary telescope for a portion of the scan mirror rotation (approximately five times the instantaneous field of view (IFOV).

2. They must not reduce (obscure) the "active" or ground scene field of view (80° total).

3. They should minimally increase the outside "envelope" of the scan head because of aircraft space limitations.

4. They must not reduce the mechanical integrity of the primary telescope.

To meet the above criteria, the "U" shaped channel, which is the basic structure of the scan head, will be inverted from its original downward orientation to an upward orientation. This allows access to a greater portion of the primary field of view without obscuring the required active portion or greatly increasing the scanner envelope. Inverting this channel has no impact on the mechanical design concept of the scan head, but does change numerous details.

The other area of the scan head requiring modification is the size of the sled which supports the spectrometer. This unit must be larger and modified to accommodate the greater size and weight of the thermal spectrometer. This modification affects the position of the thermal compensating bars controlling the movement of the sled and secondary mirror mount by moving them farther apart. As with adding the blackbodies, the concept and calculated design of the head remain unaltered, but detail changes are required.

2.1.3. THERMAL REFERENCE SOURCES

Two independent thermal reference sources are located and attached on each side of the scan head so that they fill the

field of view of the primary telescope for a portion of each scan mirror revolution. The references consist of one heat/cool bidirectional blackbody and one heated blackbody. The bidirectional blackbody is capable of raising or lowering its reference surface temperature with respect to the surrounding ambient. The heated blackbody can only raise its reference surface temperature with respect to the ambient.

Each reference surface consists of an 8 inch square, 1/4 inch thick copper plate with an exterior side finished to produce a surface emissivity near unity. For the bidirectional blackbody, this copper plate and a finned heat sink of similar dimensions are sandwiched around an array of thermoelectric heat pumps. The thermoelectric heat pumps transfer heat in either direction between the copper plate and the heat sink. The direction of the heat transfer and the amount are determined by the blackbody temperature desired and implemented through an electronic controller. For the heated blackbody, the copper plate and an insulating block of similar dimensions are sandwiched around a resistance heating element which heats the copper plate on command from its electronic controller. Thermistors embedded into each copper plate measure their temperature for monitoring and provide feedback signals to the controllers. The efficiency of the heat sink on the bidirectional blackbody is increased by forced air flow past its fins.

The energy from the heated blackbody is directed onto the focusing optics before the active ground scene and energy from the bidirectional blackbody is received by the optics after the active ground scene portion of the scan. This sequence results in air movement from the rotating mirror directing the heat produced by the warmer reference surface away from the scanner, rather than into the scanner housing where it might produce a thermal gradient within the head. Insulating materials, placed in strategic locations around each blackbody, further reduce the potential for such gradients.

2.1.4. SCAN MOTOR/MIRROR/ENCODER ASSEMBLY

The scan motor/mirror/encoder assembly is an integral part of the primary telescope, and consists of a permanent magnet direct current motor with a flat mirror attached to one end of its shaft at a 45° angle with respect to the motor spin axis. At the opposite end of the motor shaft is a precision optical encoder assembly.

The scan mirror is constructed from a beryllium substrate truncated at a 45° angle and then plated with electroless nickel, polished, coated with an aluminum reflective surface and finally receives a protective overcoat of silicon monoxide. The mirror, when viewed at an angle normal to the direction of rotation, has a circular clear aperture of 7.5". The inherent imbalance of this structure is compensated by fitting a precision machined stainless steel shroud over the mirror. This resultant assembly has the rotational forces balanced to such a degree that the mirror surface will remain flat at all rotation rates up to 25 scans/sec within 1/4 wave of sodium light. The balancing shroud also reduces abnormal wear on the bearings which might be caused by imbalance.

The encoder assembly, mounted on the scan motor shaft, serves as a position sensor for motor speed control, and the fundamental reference frequency for all system timing. The encoder assembly consists of a circular disk attached to the motor shaft, a separate assembly containing a lamp and photodetectors, and preamplifier/interface circuitry for the photodetector signals. The two signals produced by the encoder are one-pulse per revolution, used as a "start of frame" sync; and a 6000-pulses per revolution used to synchronize the system clocks and control the motor speeds.

2.2. SPECTROMETER OPTICAL DESIGN

The spectrometer optical design encompasses all of the components required to transfer and spectrally disperse the

energy collected by the primary telescope onto an array of sensors at its output. These components include a collimator, a dispersing element, and a focusing optic. The sensor array is included in this section, because it is an integral part of this design. All optics in the spectrometer must have uniform or predictable spectral characteristics and high efficiency across the 8 to 13 μm wavelength range.

A fundamental requirement for an airborne scanner used to collect multispectral data is that the IFOV be simultaneously imaged on all spectral detectors. The degree of optical complexity needed to accomplish this task is determined by the number of detector types for the IR spectral bands, accuracy of spectral purity, overall physical size, and reliable operation to meet mission requirements. Only one detector type is needed for the specified spectral bands.

Spectral purity has not been rigorously defined by contract. However, during an interim meeting with the sponsor a working definition was presented that is based on a triangular slit function and allows approximately 50% mixing of spectral energy in adjacent channels. This working definition is commonly used as a design goal in spectrometer systems desiring continuous spectral coverage*. Sufficient experimental data is not available to determine with certainty that this spectral purity is adequate for the intended applications of the instrument.

2.2.1. COLLIMATOR

Diffraction from the collimator aperture must be minimized by using a large diameter optic; however, this choice must be constrained by overall system size. A reasonable compromise is to make the collimator 1/2 the size of the primary parabola. With this starting point, a collimator of 3.75" diameter and a focal length of 6.5" was studied.

*The MSDS 24 channel scanner system, which parallels the TIMS scanner in function, used this working definition for its initial design. This design was later modified by the addition of bandpass filters over each detector element.

The important optical aberrations to consider for a first design phase are third order spherical and coma. Both aperture size and total field angle determine the magnitude of these aberrations. Aperture size must be matched to the f/N of the primary parabola for maximum energy collection. The field angle is fixed by the collimator focal length and the field stop size. The 2.5 mrad IFOV and a primary focal length of 13" (330.20 mm) yields a field stop size of 0.0325" (0.8255 mm) square. This results in a collimator FOV of 7.1 mrad across the diagonal of the square.

Good image quality can be maintained if the collimator aberrations do not exceed 1 mrad. Poor image quality would degrade both the system sensitivity and spectral resolution. Another important sensitivity consideration is optical efficiency or throughput of the collimator. A simple review of suitable optics is tabulated in Table 1 with an indication of overall spectrometer length.

TABLE 1. COLLIMATOR TRADE-OFF CONSIDERATIONS

OPTICAL TYPE	BLUR CIRCLE	EFFICIENCY	OVERALL LENGTH
Single Lens	1.65 mrad	0.95	14
Mirror Sphere	1.70 mrad	0.98	7
Mirror Parabola	0.15 mrad	0.98	7

Based on the data from Table 1, a parabolic reflective collimator design was selected.

2.2.2. DISPERSIVE ELEMENT

System size is significantly affected by the optical method used to separate the six spectral bands. For the defined spectral purity, this separation may be accomplished with either prisms or a grating. System reliability is best accomplished by designing a simple optical configuration with the minimum number of components placed compactly in a stable housing. Prisms were eliminated from consideration for two

reasons: 1) sodium chloride (NaCl) which is the only optical material with sufficient dispersion, transmission, mechanical stability, and availability is hydroscopic; and 2) more than one prism would be needed for the required dispersion, reducing optical efficiency and increasing mechanical complexity. For these reasons, a grating was selected as the dispersing element.

Based on the final spectral band definition, tables were prepared as a function of groove spacing and diffraction order. Only the +1 and -1 orders were considered as providing adequate grating efficiency for the required system sensitivity. Results of these calculations are shown in Tables 2-7. The blaze angle will be specified based on results of the sensitivity analysis in Section 2.4.

The -1 order was eliminated as a design alternative because of the large tilt angle for the detector dewar and imaging lens. This angle places the top of the dewar outside the envelope of the basic scanner and would make routine filling of the dewar difficult. The calculations of the -1 order are included for completeness. From these tables and knowing that the detector size desired is near 0.015", it can be deduced that the grating should have 12 or 13 grooves/mm. Discussions with Bausch & Lomb restricted our design to a 12 grooves/mm grating due to the limitation of available gearing for ruling engines.

Grating efficiency is controlled by several factors including surface micro roughness, coating reflectivity, polarization, and blaze angle[1]. Figure 3 shows the measured efficiency of a 20 g/mm grating plotted vs wavelength. The operating wavelength is similar to the TIMS design with a slightly greater blaze angle of 5.06°. Based on past experience, Bausch & Lomb has quoted a peak efficiency of 90% for a 12 g/mm grating blazed near 3°. The explanation of slightly improved efficiency is due to wider groove widths and small blaze. Coarse gratings with small blaze angles exhibit minimal polarization effects[2]. Scaler theory accurately predicts

TABLE 2. DIFFRACTION GRATING DATA: 11 Grooves Per Millimeter +1 Order

	WAVELENGTH *(micrometers)*	DIFFRACTION *(degrees)*	DISPERSION *(milliradians)*	BAND SIZE *(inches)*	BAND SIZE *(millimeters)*	BLAZE ANGLE *(degrees)*
Band 1	8.2 - 8.6	19.4156 - 19.1485	4.66147	0.0138	0.350	2.79
Band 2	8.6 - 9.0	19.1485 - 18.8819	4.65399	0.0137	0.349	2.93
Band 3	9.0 - 9.4	18.8819 - 18.6156	4.64657	0.0137	0.348	3.06
Band 4	9.4 - 10.2	18.6156 - 18.0844	9.27144	0.0274	0.695	3.19
Band 5	10.2 - 11.2	18.0844 - 17.4227	11.5502	0.0341	0.866	3.46
Band 6	11.2 - 12.2	17.4227 - 16.7633	11.5084	0.0340	0.863	3.79

TABLE 3. DIFFRACTION GRATING DATA: 12 Grooves Per Millimeter +1 Order

	WAVELENGTH *(micrometers)*	DIFFRACTION *(degrees)*	DISPERSION *(milliradians)*	BAND SIZE *(inches)*	BAND SIZE *(millimeters)*	BLAZE ANGLE *(degrees)*
Band 1	8.2 - 8.6	18.9182 - 18.6277	5.0697	0.0150	0.380	3.04
Band 2	8.6 - 9.0	18.6277 - 18.3378	5.06106	0.0149	0.380	3.19
Band 3	9.0 - 9.4	18.3378 - 18.0483	5.0526	0.0149	0.379	3.33
Band 4	9.4 - 10.2	18.0483 - 17.4707	10.0804	0.0298	0.756	3.48
Band 5	10.2 - 11.2	17.4707 - 16.7513	12.5559	0.0371	0.942	3.76
Band 6	11.2 - 12.2	16.7513 - 16.0346	12.5086	0.0369	0.938	4.12

TABLE 4. DIFFRACTION GRATING DATA: 13 Grooves Per Millimeter +1 Order

	WAVELENGTH *(micrometers)*	DIFFRACTION *(degrees)*	DISPERSION *(milliradians)*	BAND SIZE *(inches)*	BAND SIZE *(millimeters)*	BLAZE ANGLE *(degrees)*
Band 1	8.2 - 8.6	18.4223 - 18.1085	5.47594	0.0162	0.411	3.29
Band 2	8.6 - 9.0	18.1085 - 17.7954	5.4661	0.0161	0.410	3.45
Band 3	9.0 - 9.4	17.7954 - 17.4827	5.45654	0.0161	0.409	3.60
Band 4	9.4 - 10.2	17.4827 - 16.859	10.8852	0.0321	0.816	3.76
Band 5	10.2 - 11.2	16.859 - 16.0823	13.5564	0.0400	1.017	4.07
Band 6	11.2 - 12.2	16.0823 - 15.3086	13.5036	0.0399	1.013	4.46

TABLE 5. DIFFRACTION GRATING DATA: 10 Grooves Per Millimeter -1 Order

	WAVELENGTH *(micrometers)*	DIFFRACTION *(degrees)*	DISPERSION *(milliradians)*	BAND SIZE *(inches)*	BAND SIZE *(millimeters)*	BLAZE ANGLE *(degrees)*
Band 1	8.2 - 8.6	30.306 - 30.5718	4.63951	0.0137	0.348	2.65
Band 2	8.6 - 9.0	30.5718 - 30.8384	4.6522	0.0137	0.349	2.79
Band 3	9.0 - 9.4	30.8384 - 31.1057	4.66514	0.0138	0.350	2.92
Band 4	9.4 - 10.2	31.1057 - 31.6425	9.37015	0.0277	0.703	3.05
Band 5	10.2 - 11.2	31.6425 - 32.318	11.7893	0.0348	0.884	3.32
Band 6	11.2 - 12.2	32.318 - 32.9986	11.878	0.0351	0.891	3.66

TABLE 6. DIFFRACTION GRATING DATA: 11 Grooves Per Millimeter -1 Order

	WAVELENGTH *(micrometers)*	DIFFRACTION *(degrees)*	DISPERSION *(milliradians)*	BAND SIZE *(inches)*	BAND SIZE *(millimeters)*	BLAZE ANGLE *(degrees)*
Band 1	8.2 - 8.6	30.8517 - 31.1458	5.13321	0.0152	0.385	2.93
Band 2	8.6 - 9.0	31.1458 - 31.4409	5.14907	0.0152	0.386	3.07
Band 3	9.0 - 9.4	31.4409 - 31.7368	5.1654	0.0153	0.387	3.22
Band 4	9.4 - 10.2	31.7368 - 32.3316	10.3806	0.0307	0.779	3.37
Band 5	10.2 - 11.2	32.3316 - 33.0806	13.0728	0.0386	0.980	3.67
Band 6	11.2 - 12.2	33.0806 - 33.836	13.185	0.0389	0.989	4.04

TABLE 7. DIFFRACTION GRATING DATA: 12 Grooves Per Millimeter -1 Order

	WAVELENGTH *(micrometers)*	DIFFRACTION *(degrees)*	DISPERSION *(milliradians)*	BAND SIZE *(inches)*	BAND SIZE *(millimeters)*	BLAZE ANGLE *(degrees)*
Band 1	8.2 - 8.6	31.4006 - 31.7233	5.6333	0.0166	0.422	3.20
Band 2	8.6 - 9.0	31.7233 - 32.0472	5.65302	0.0167	0.424	3.36
Band 3	9.0 - 9.4	32.0472 - 32.3723	5.67299	0.0168	0.425	3.52
Band 4	9.4 - 10.2	32.3723 - 33.0259	11.4081	0.0337	0.856	3.69
Band 5	10.2 - 11.2	33.0249 - 33.8498	14.3802	0.0425	1.079	4.01
Band 6	11.2 - 12.2	33.8498 - 34.6818	14.5204	0.0429	1.089	4.42

efficiency for diffraction and blaze effects; however, surface reflectivity must be determined by direct measurement[2]. Based on this evidence, sensitivity calculations shall use a peak grating efficiency of 90% and a universal efficiency curve shown in Figure 4[3].

During the initial design phase, consideration was given to minimizing the incident and diffracted angles in order to reduce polarization effects. In this type of design, the collimated beam would be incident to the grating's nondispersive axis and diffraction would be out of the plane of incidence. As information was gathered from three grating manufacturers, it becamse clear that polarization problems were insignificant at 12 g/mm in the 8-13 μm wavelength region. The optical design was finalized using the grating in a standard Littrow configuration. This decision simplified the mechanical design and optical alignment complexity.

A master grating shall be fabricated on an aluminum blank and the delivered grating(s) shall be replicas made of Zerodur® substrate coated with evaporated aluminum and protected by a thin overcoat of silicon monoxide. A low thermal expansion grating substrate is required for spectrometer stability over the specified operational temperature extremes.

Spectral purity or "wavelength crosstalk" is graphed in Figure 5. These spectral slitwidths are proportional to the convolution of the field stop image and the detector edge boundaries. Boundary edges are measured in the direction of dispersion and gaps are illustrated. The spectral slitwidth will appear as a triangle when the field stop image is equal to a detector width and as an equal angle trapezoid for greater or lesser detector widths.

The wavelength labels at the trapezoid tops and the triangle peaks indicate when the detector element is fully filled by the geometric image of the field stop. The wavelength labels at the bases indicate when the field stop image

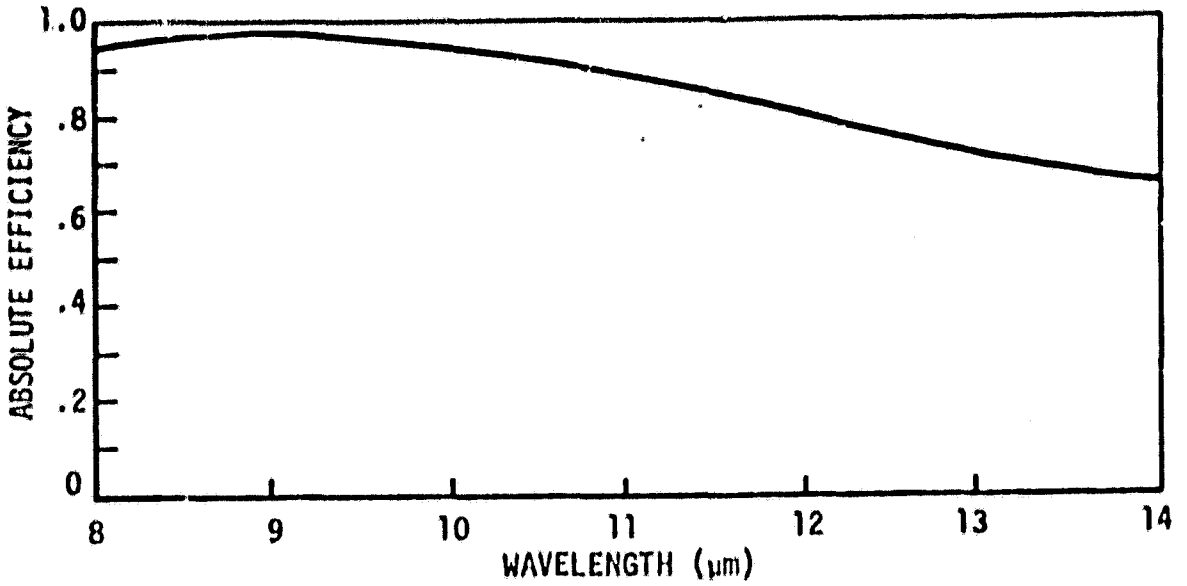

FIGURE 3. EFFICIENCY OF A 20 g/mm GRATING

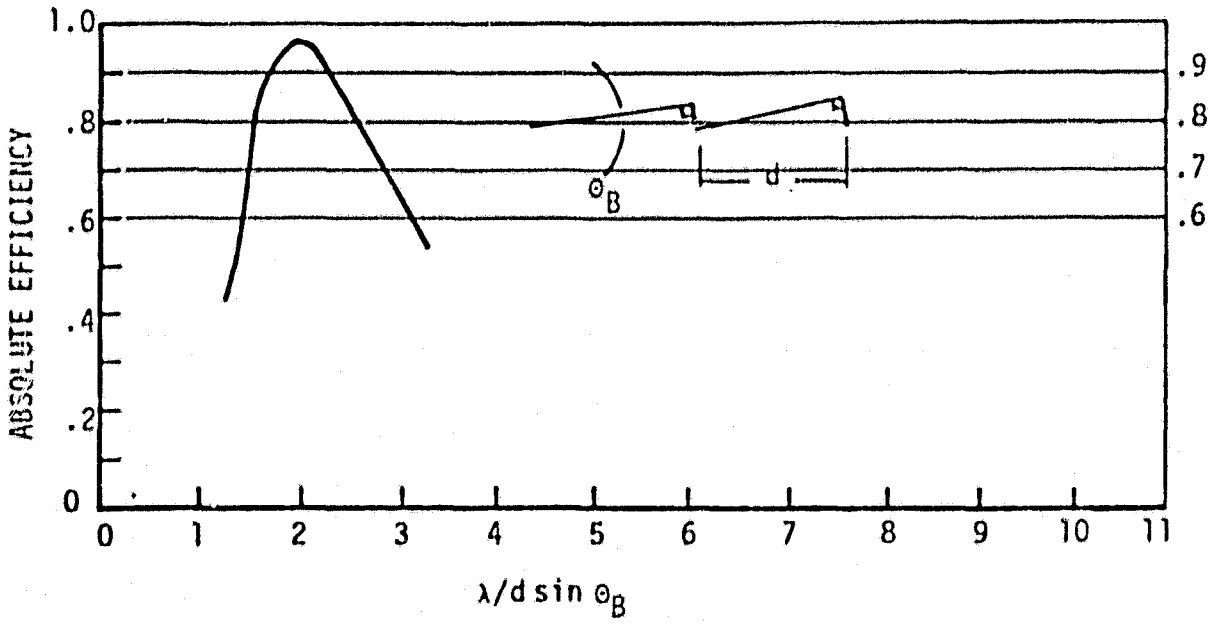

FIGURE 4. UNIVERSAL GRATING EFFICIENCY CURVE

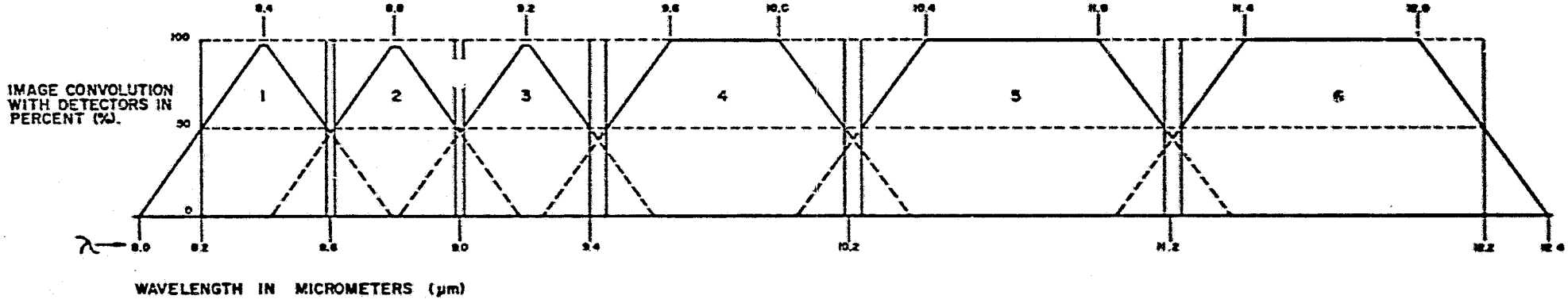

FIGURE 5. SPECTRAL SLIT WIDTHS FOR SIX BANDS

first crosses a detector edge boundary from either direction. Graphs of this type may be constructed to include diffraction and aberration image spreading, but do not produce additional insight into final system performance. Additional effects on spectral purity of these and other image defects are included in Section 2.2.3. The shape of the graph will also be affected by spatial variations of detector responsivity.

2.2.3. OPTICAL LAYOUTS

Two basic configurations were considered: 1) an axial paraboloid collimator used with a grating that has a hole through its center; and 2) an off-axis paraboloid. These configurations are shown schematically in Figure 6.

Other layouts were investigated and, in general, two common problems arose: 1) additional optical elements were needed; and 2) there was insufficient mechanical clearance for use with the existing scan head design. None of these layouts had a definite advantage that would warrant changing the basic scan head. Both the axial mount and off-axis mount share several common features:

1. Optical aberrations are identical.
2. Grating may be used in +1 or -1 order.
3. Diffracted beam is accessible from both in-plane and out-of-plane dispersion.
4. Mechanical interface difficulties are equal.
5. Grating incident angle is the same.

Further investigation found that the axial mount had two disadvantages. The first problem was in fabricating a central hole in the grating. One manufacturer, Instruments S.A., advised that there could be a phase difference in the ruling across the hole. In addition, the cost of fabricating a conical central hole was substantial. The second problem was that the detectors could directly view the field stop through the central hole. This geometry begins to appear like a blackbody cavity whose back surface is the field stop. The unknown question is,

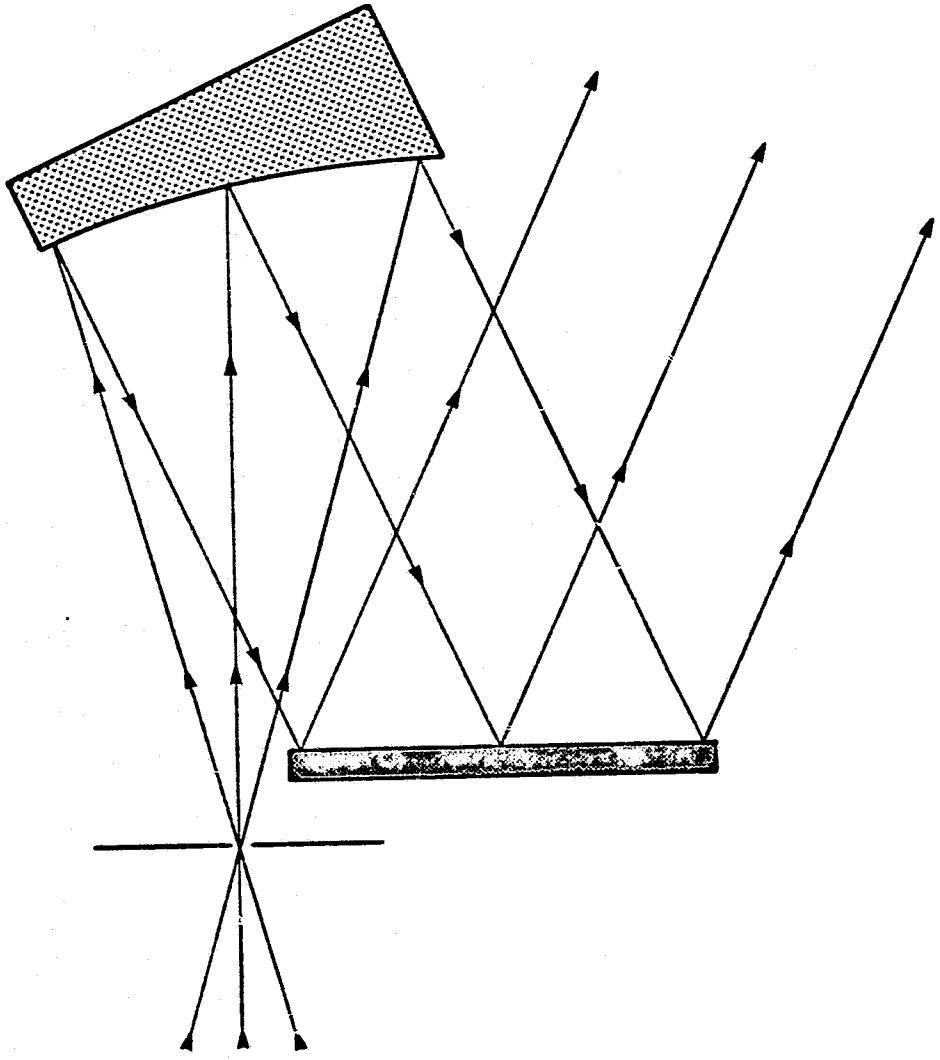

OFF-AXIS PARABOLOID

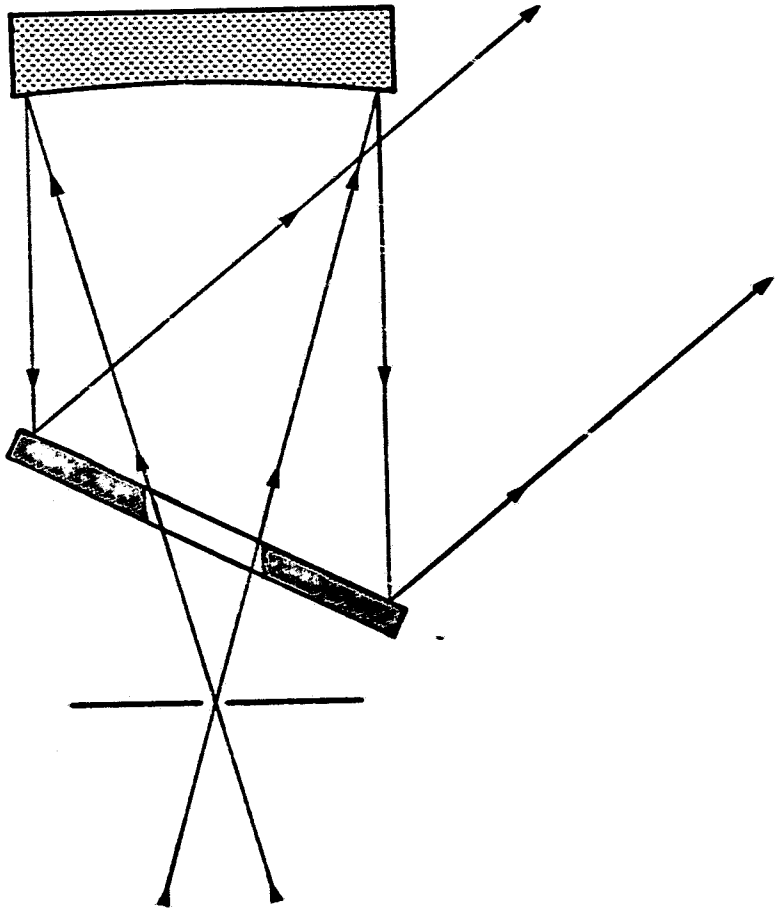

AXIAL PARABOLOID

FIGURE 6. OPTICAL LAYOUTS

what temperature modulation could be expected from scan mirror pumping on the field stop? Shorter wavelength spectrometers are not affected by this source of stray radiation. However, for thermal IR instruments modulated housing backgrounds can increase system noise to a level that makes data recovery impossible. Because of these problems, further analysis of the axial mount was discontinued.

The major difficulty with the off-axis mount is cost, both in fabrication of the larger paraboloid and the increased complexity of alignment. These penalties are acceptable when compared to the alternatives. A full mechanical layout (see Figure 11) shows that the off-axis spectrometer is compatible with the existing scan head.

2.2.4. FOCUSING OPTIC

From past experience and manufacturers' performance data a basic design goal was to keep the detector element sizes small. Choosing the smallest detector to be 0.015" square and using the spectral purity definition requires that the field stop image be demagnified by the ratio of 2.167:1 (0.0325/0.015). This requires a focal ratio of 0.8 for the focusing optic. With the smallest detector 0.015" square, the total array length for the six channels becomes 0.150". Based on a collimator focal length of 6.5", the focusing optic focal length is 3.0" (6.5/2.167) with an angular field coverage of $\sim 3°$ ($\pm 1.43°$). To hold design time and cost to a minimum, a vendor search was made for a suitable lens. An f/0.62 75 mm EFL (2.953") three element germanium lens is available from Research Optics. From this information, it was decided to use this standard lens and alter the collimator focal length slightly to achieve the desired demagnification ratio.

A commercially available f/0.62, 75 mm EFL three element germanium lens will be used to refocus diffracted energy onto the detector array. Each lens surface shall be anti-reflection coated to reduce optical losses caused by the high refractive

index of germanium. Figure 7 shows transmission through anti-reflection coated plano germanium plates. The HEA® coating is a trademark of Optical Coating Labs, Inc. and is an indication of the performance to be expected. Average transmission for each element may be conservatively estimated at 95%. Another transmission loss in germanium is caused by electron-free carrier absorption. This loss increases with lens temperature. It may also be related to a number defined as emissivity and has a value of 0.002 at 25°C. The lens not only absorbs incident radiation, it also emits blackbody energy and increases background radiation viewed by the detector.

Further energy loss is caused by imperfect imaging of the field stop onto the detector elements. These imperfections may be separated into two types: diffraction and geometric. Both types of defects cause the image to spread, thereby reducing energy concentration onto detector elements. Diffraction may be reduced to a reasonable level by using large aperture optics. Geometric or aberrational defects are controlled by lens material along with surface radii and thickness. Figure 8 shows image diameter as a function of focal plane position and the diffraction spread at two wavelengths. Diffraction size is plotted for both 84% and 95% energy content. The expanding conical section is the envelope of chromatic aberration caused by germanium's dispersion. All other lens aberrations are insignificant compared to the chromatic spread. Additional geometric image defects are shown in spot diagrams (see Figure 9). Each of these diagrams is made up of 65 points, traced to a focal plane near 9 μm. Some points are concentrated into a large central point. An improvement in image quality is possible if the detector array is tilted around its midpoint: .001" toward the lens for 8.2 μm and .001" away for 12.2 μm[5].

Further image degradation can be expected from defocusing. Because of the large focusing angle (38° half angle), focal shifts should not exceed 0.0005". Figure 8 graphically depicts

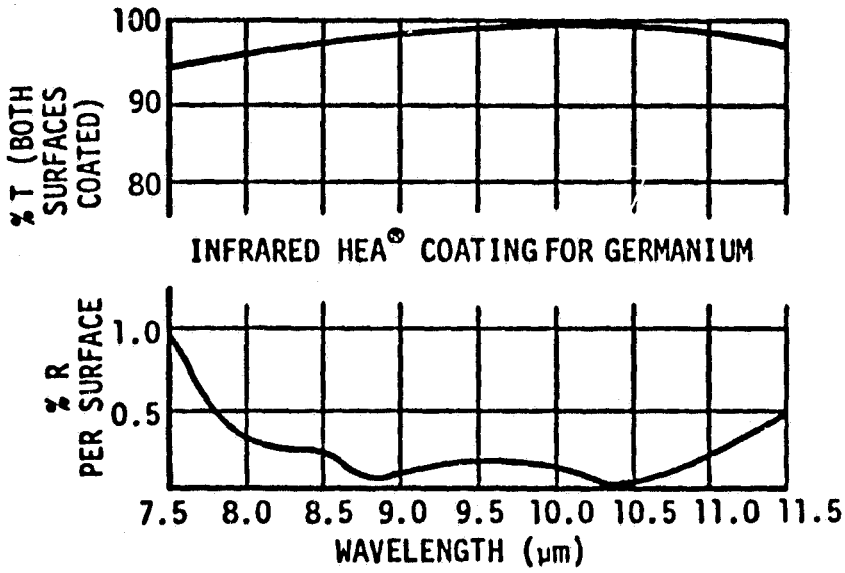

FIGURE 7. ANTI-REFLECTION COATING PERFORMANCE ON GERMANIUM

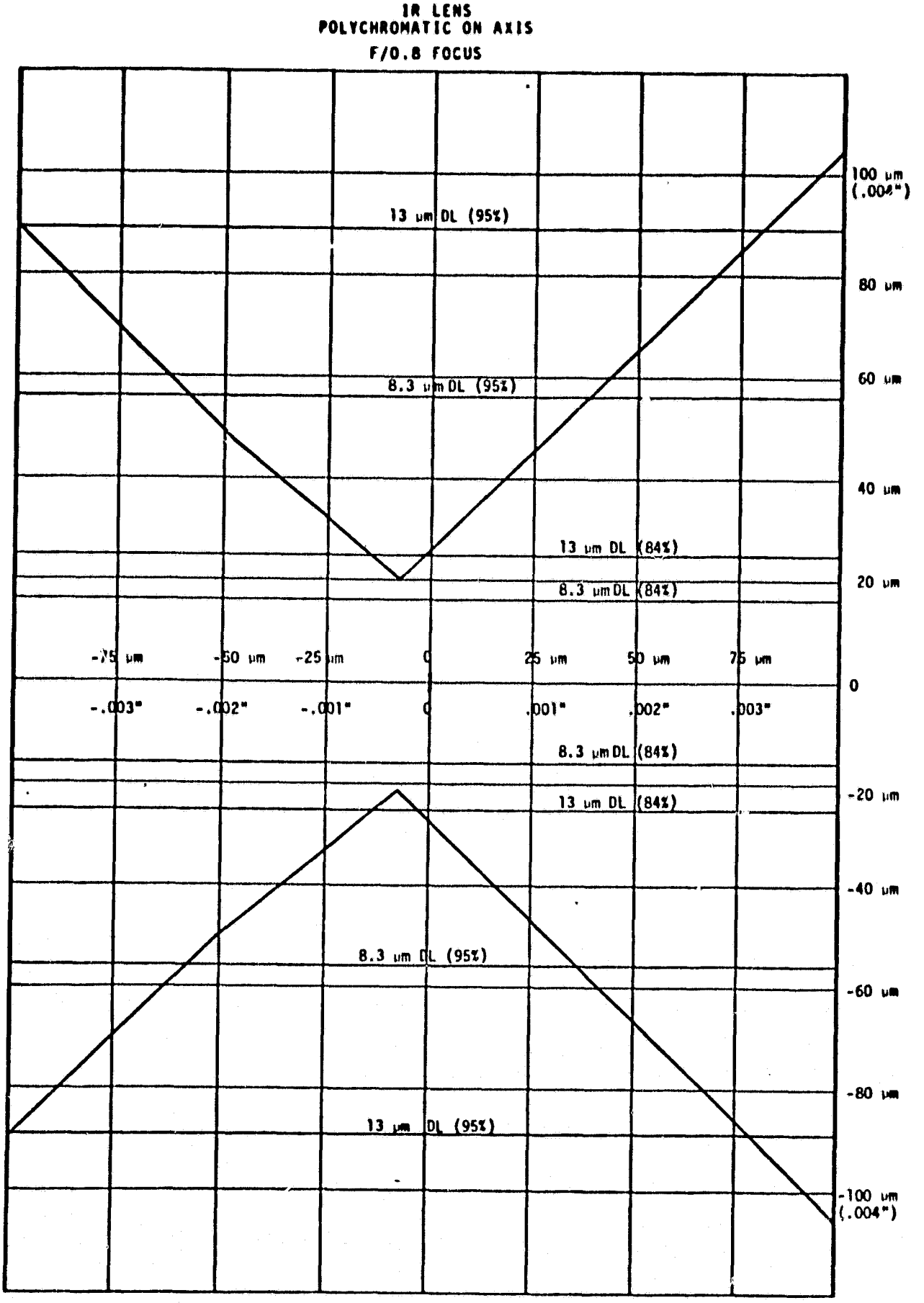

FIGURE 8. IMAGE DIAMETER VS FOCAL PLANE POSITION

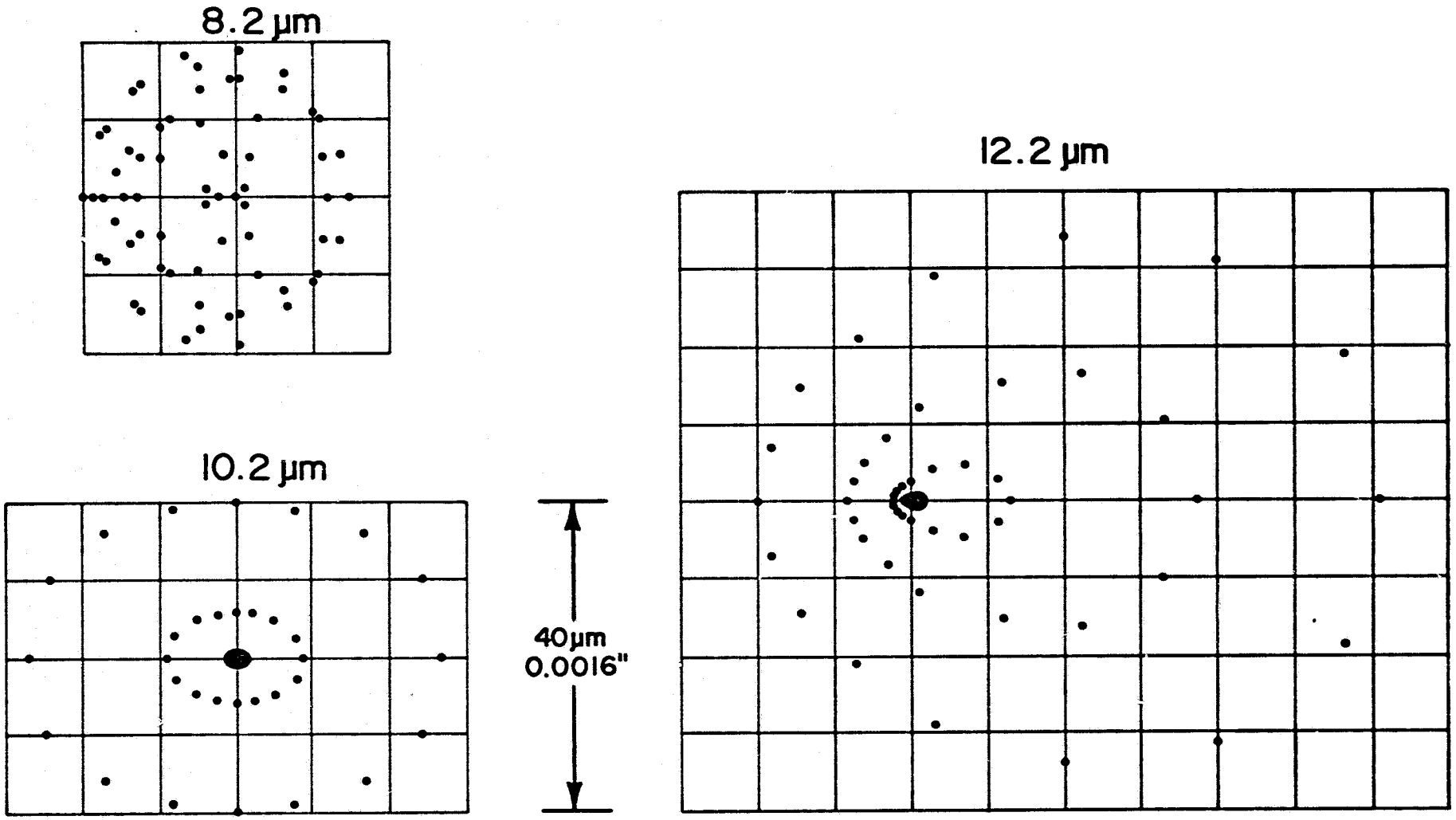

FIGURE 9

SPOT DIAGRAM OF 65 RAYS FROM CENTER OF FIELD
STOP FOR THREE DIFFRACTION ANGLES

the magnitude of this problem. Once this best focal position is obtained, it must be maintained over the operating temperature range. Temperature compensation techniques must be used for both optical and mechanical variations.

Optical temperature focal shifts are caused by changes in refractive index, lens surface radii, lens thickness, air space separation, and most important the lens mount. Research Optics has been advised of the lens performance requirements over the specified temperature range. They have previously produced temperature compensated lens assemblies. The procedure they described is to use modulation transfer function (MTF) measurement equipment to determine focal plane performance as the lens is temperature cycled. Using a sliding barrel, one of the lens elements will be allowed to move in a manner that maintains a constant focal position over temperature. Their representative explains that the refractive index temperature change of germanium is not consistent from one blank to the next. Therefore, experimental methods must be used to "hand tune" each lens assembly.

The temperature compensated focal position shall be maintained with respect to a fixed reference surface of the lens barrel. Additional temperature compensation will be used to keep the detector/dewar at the lens focus. Detector array movement within the dewar will be controlled partially by holding the internal dewar temperature constant over altitude extremes. This will be accomplished by means of a pressure valve on the dewar nitrogen chamber. Any remaining movement of the detector plane will be compensated in the dewar mount.

The effect of these image defects is most severe in the short wavelength bands of the spectrum, and results in reduced system sensitivity and a slightly lower MTF. Spatial resolution can be predicted on the basis of spot diagrams to be greater than 80% modulation for a 2.5 mrad IFOV in the short wavelength bands. This modulation would improve for the larger detectors.

Spectral slitwidth appearance will be altered in the actual instrument from that shown in Figure 5. Because the central core of the image contains less energy, the band edges will rise faster and the tops will be rounded. This effect will narrow each spectral bandwidth slightly.

2.2.5. DETECTOR ARRAY AND DEWAR ASSEMBLY

If there is one single item that could be called the most important in a system such as this, it would be the detector array and dewar assembly. A major concern in this study was to specify high performance from the sensors while not attempting to advance the state of the art in detector manufacturing and packaging. All system parameters remained flexible until the array specifications could be finalized and its limitations known.

Mercury-cadmium-telluride (MCT) is clearly the material of choice for each of the six sensors. However, an option still remained between two types of MCT: photoconductive (PC) and photovoltaic (PV). The technology of producing high performance PV MCT detectors is relatively new. The (theoretical) advantages of the PV MCT detector compared to the PC MCT detector are: 1) higher speed; 2) no bias current requirement; 3) lower power dissipation; 4) lower 1/f noise; and 5) lower "generation-recombination" noise. Of these five potential advantages, #1 and #3 are not significant for this application.

The technique of producing high performance PC MCT detectors is mature and well known among a limited number of high technology manufacturers. The advantages of the PC MCT detector compared to the PV MCT detector are: 1) lower cost; 2) shorter delivery; 3) lower risk; and 4) better uniformity of response across the array and across the larger individual elements of the array.

The PC MCT was selected over the PV MCT primarily because of advantages #1, #2 and #3 above, which are all inter-related.

In spite of the theoretical advantages of PV MCT over PC MCT, there is no clear performance difference between these two types when comparing detectors that have actually been built and tested, or when comparing performance specifications that vendors are willing to quote. The chances of producing a high performance array, in a timely fashion, are excellent with PC MCT and questionable with PV MCT.

Table 8 summarizes the methods that were considered for fabricating the detector array.

The overall optical design of the secondary optics produces a demagnification of the system field stop of approximately 2. This is done to keep the detector area as small as practical to minimize any degradation in system sensitivity due to sensor noise. The small detector size requires high precision in the physical dimensions of the array. Since all of the wavelength band edges are specified to be contiguous, it becomes important to keep the space between elements small so that this specification can be closely approximated in practice, and so that a minimal amount of energy falls onto inactive areas of the array. After close liaison with vendors, the dimensions as shown in Figure 10 were specified. These dimensions permit the array to be built from two three-element monolithic sections, dividing between elements 3 and 4. The 0.002" gap specified between elements 3 and 4 is enough working space to join the two arrays. The section of the array consisting of elements 4, 5 and 6, although intended to be monolithic, could upon completion of the array include one or more discrete elements. This may be necessary because of the high performance required from each element, and the uncertain response uniformity over a detector area as large as these three elements combined. A gap of 0.002" between these elements permits the array supplier to cut-out and replace elements in this section if necessary.

TABLE 8. DETECTOR ARRAY FABRICATION METHODS

	ADVANTAGES	*DISADVANTAGES*
1. One 6-element monolithic array	1. Narrow, precise gaps between elements 2. Well defined band edges	1. Optimum D* performance for 1 or 2 elements only
2. Six individual elements assembled into array	1. Optimum D* performance for all six elements	1. Large and imprecise gaps between elements 2. Band edges less well defined
3. One 4-element monolithic array and one 2-element monolithic array	1. Might use multiple grating orders	1. Wider FOV required from imaging lens 2. A 20% efficiency loss in 2nd grating order
4. Two 3-element monolithic arrays	1. Precise gaps between most elements 2. Well defined band edges 3. Optimum D* performance for most of the elements	

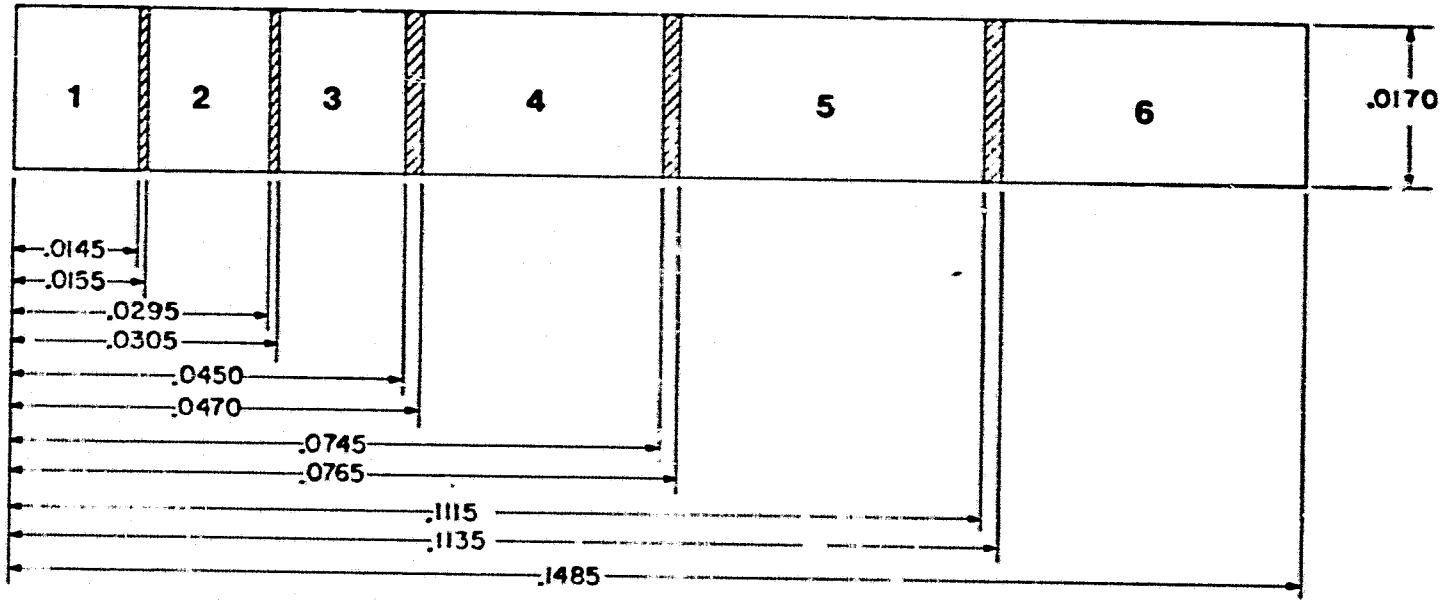

REVISIONS

SYM	DESCRIPTION	BY	DATE

ALL .XXX DIMENSIONS ± .0005 TOLERANCE

NOTES:

Daedalus Enterprises Inc.

DWG. NO. 190B001-A

PART NUMBER MTTIMSIA

TITLE TIMS DETECTOR ARRAY

SCALE 10:1

TOLERANCES UNLESS OTHERWISE SPECIFIED

.01 .005

FIGURE 10. TIMS DETECTOR ARRAY (MECHANICAL LAYOUT)

The calculated width (the undispersed dimension) of the array is 0.015". To this width has been added 0.002". This added margin of sensitive area ensures that most of the energy at the detector plane is collected by the sensors, allowing tolerances in the focal lengths of the secondary optics (magnification ratio), and allowing small alignment errors or slight misalignment across the operating temperature range. This added margin also eliminates reflection of the small amount of energy hitting the array plane on the gold contact strips which are outside the active area.

The LN_2 dewar is an all stainless steel pour-fill design. It is preferred over a glass dewar with aluminum jacket principally because of its superior and predictable mechanical stability at the array plane over the temperature range required. A pour-fill rather than a closed cycle cryogenic supply system was selected because of its simplicity and inherent reliability. The dewar will have a low pressure relief cap to reduce temperature variations of the LN_2 as a function of operating altitude. The dewar will require periodic re-evacuation to maintain the required LN_2 hold time. The dewar will contain an internal temperature sensor to detect the absence of LN_2 and will permit a protective circuit to be incorporated which will remove or inhibit the detector bias current and, therefore, eliminate potential damage to the array. As an additional protective measure, the detector bias is produced from a high impedance current source which is "self limited" to bias power levels near the operating point selected.

Specifications for a cooled bandpass optical filter are also included with the array/dewar assembly. The purpose of the cold filter is to block radiation outside the grating's first order and to eliminate background radiation onto the detector elements at wavelengths shorter than approximately 7 μm.

2.2.6. COLD STOP

Because the detector can directly view the scanner secondary mirror, its mount and other support structures, an auxiliary optical system to reimage these supports was investigated. This image would be blocked by a cold aperture having transparent portions matching the reflecting surfaces of the primary optics. This would require a separate dewar and two windows in addition to at least two mirrors used for reimaging. This concept was abandoned early in the design study because of increased system complexity, reduced optical throughput, and the detector would still view the spectrometer housing. The addition of the cold stop would degrade rather than enhance the overall system performance. Some of the potential benefits of a cold stop can be achieved by using the cooled optical bandpass filter directly over the detector elements. Refer to the description of the detector array/dewar assembly for a discussion of this option.

2.2.7. CONVERSION TO A 6 CHANNEL 1-2.5 μm SPECTROMETER

Routine conversion of the TIMS spectrometer itself, to measure other portions of the wavelength spectrum, is not recommended because of the magnitude of the recalibration task required after conversion. It is possible, however, to convert the TIMS system to a 6 channel spectrometer in the 1-2.5 μm wavelength region, or other wavelength regions for which a suitable spectrometer can be built. However, the design of a spectrometer for wavelengths other than 8-13 μm was not investigated for this project.

Conversion to other spectrometers is possible because the design of the TIMS spectrometer is rather independent of the primary scanning system. The optical interface is at the field stop and the mechanical interface is the thermally compensated sled on which the spectrometer is mounted and which attaches to the scan head. By removing the entire spectrometer,

with its field stop and mounting sled as one unit, reinstallation of this assembly onto the scan head may be accomplished without recalibration. The spectral reflectance performance of the primary optics is high and the quality of the optical surfaces exceeds requirements for a 2.5 mrad system at any wavelength between 0.4 μm and 14 μm.

To convert the system to collect other wavelength bands would require removing the thermal infrared spectrometer assembly, including its field stop and sled, and installing a replacement spectrometer assembly with new sled and field stop. Because the field stop is positioned on the primary optical axis with locating pins, it is possible to exchange spectrometers on the scan head without an alignment procedure after such a procedure had initially been performed for each unit.

2.2.8. ADAPTING THE TIMS SPECTROMETER TO THE BENDIX 24 CHANNEL SCAN HEAD

This study investigated the use of the MSDS 24 channel scanner system as the primary collecting optics for the TIMS spectrometer, and concluded that the adaptation is not feasible. The main drawbacks to the use of this scan head are practical rather than theoretical. Its large size (approximately 6' sq x 3' high), weight (approximately 600 lbs), and high motor power requirements combine to make it incompatible with small or medium sized aircraft. The optical encoder on the motor shaft is of low resolution and accuracy compared with the one proposed for TIMS. In addition, its long primary focal length and f/5 telescope produce a field stop that is 0.090" sq for a 2.0 mrad IFOV. An optical demagnification of 6X is required in the spectrometer in order to produce an image size at the detector plane that is compatible with the sensors as defined for the TIMS system. The small size of this array is important for maximum performance of the system.

The Dall Kirkham primary telescope design used in the 24 channel scanner is relatively sensitive to movement of the optical surfaces. Because of this, it was designed for operation in a restricted thermal environment. Finally, the scan head is known to be in a disassembled and probably nonrecoverable state.

2.3. SPECTROMETER MECHANICAL DESIGN

The spectrometer mechanical design is defined as encompassing all of the components needed to 1) support and locate the optical elements in their proper positions; 2) provide the alignment of these elements after assembly; 3) provide the environmental security necessary to prevent physical damage to the elements; and 4) maintain the location of the elements over the full range of environmental conditions. Additionally, an effort was made to accomplish this task with as simple an implementation as practical. The resultant design includes a combination of aluminum and Invar steel mounting plates incorporated into a mechanical package that can be environmentally sealed when not in operation. The optical elements and their mounts are configured to be thermally compensated and also rugged enough to withstand the environment of an unpressurized aircraft. The alignment of the system has been carefully considered and provisions have been made for a laboratory procedure to accomplish this. Each of these four design criteria will be discussed in this section and a drawing of the completed assembly is shown in Figure 11. NOTE: With regard to material selection, all components are 6061T6 aluminum unless otherwise stated and all Invar steel is Carpenter "Invar 36".

2.3.1. SUPPORT AND LOCATION OF THE OPTICAL ELEMENTS

The spectrometer mechanical design was concerned with the location of the following items: 1) the field stop aperture; 2) the collimating mirror; 3) the diffraction grating; 4) the imaging lens; and 5) the detector/dewar package. Each of these elements requires a custom mounting arrangement.

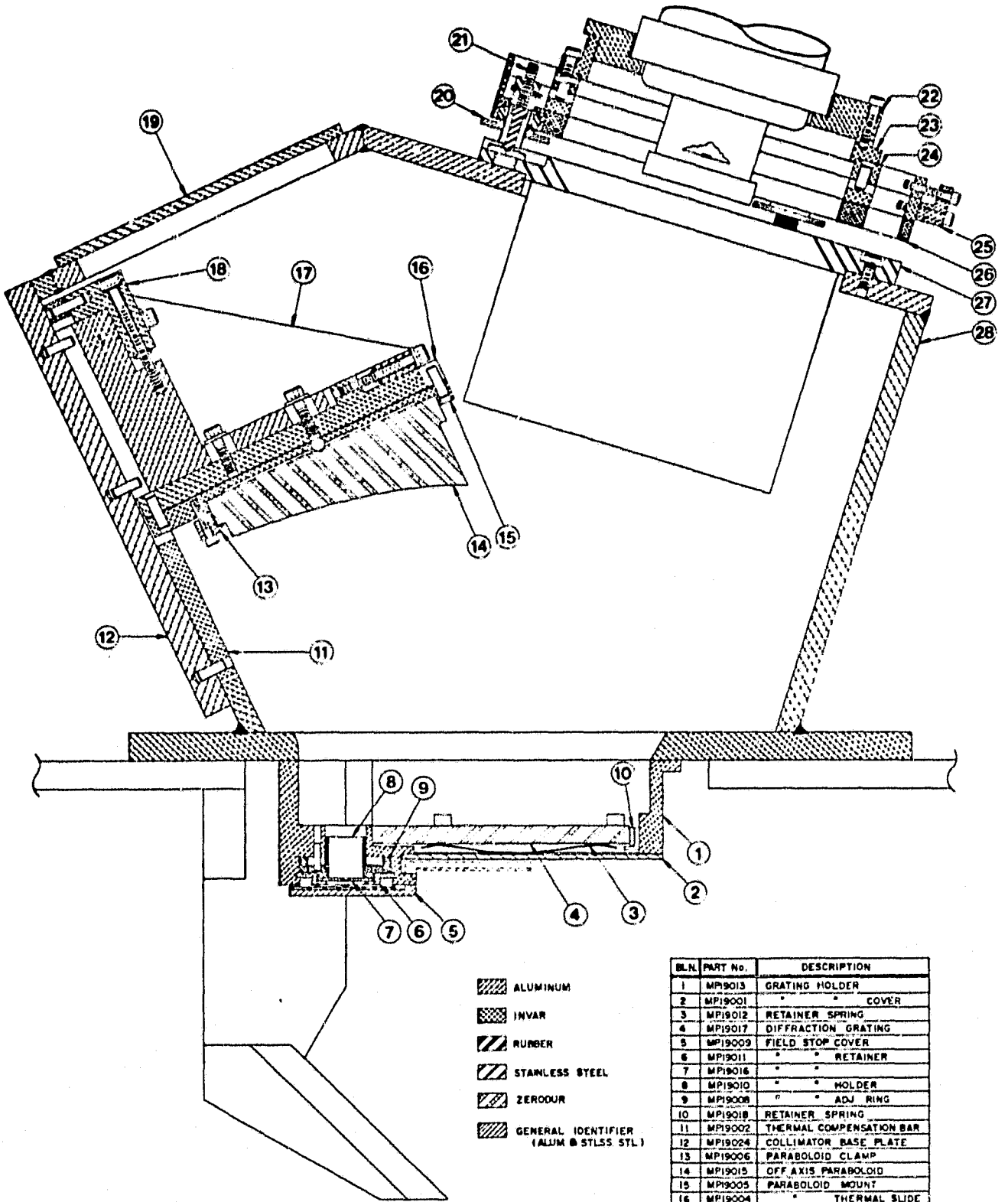

BLN.	PART No.	DESCRIPTION
1	MP19013	GRATING HOLDER
2	MP19001	" " COVER
3	MP19012	RETAINER SPRING
4	MP19017	DIFFRACTION GRATING
5	MP19009	FIELD STOP COVER
6	MP19011	" " RETAINER
7	MP19016	" "
8	MP19010	" " HOLDER
9	MP19008	" " ADJ RING
10	MP19018	RETAINER SPRING
11	MP19002	THERMAL COMPENSATION BAR
12	MP19024	COLLIMATOR BASE PLATE
13	MP19006	PARABOLOID CLAMP
14	MP19015	OFF AXIS PARABOLOID
15	MP19005	PARABOLOID MOUNT
16	MP19004	" THERMAL SLIDE
17	MP19014	COLLIMATOR BASE
18	MP19007	PARABOLOID BASE CLAMP
19	MP19023	COLLIMATOR ACCESS COVER
20	MP19032	PRZ ADJ WHEEL
21	MP19031	ADJ POST
22	MP19021	DEWAR MOUNTING PLATE
23	MP16320	ROTATION ADJ PLATE
24	MP19018	'X' AXIS " "
25	MP19019	'Y' AXIS " "
26	MP19003	ROLL/PITCH PLATE
27	MP19022	LENS ASSEMBLY
.8	AC19001	HOUSING

FIGURE 11. SPECTROMETER ASSEMBLY

2.3.1.1. FIELD STOP. The aperture plate is fabricated from a nickel plate .001" in thickness which is chemically etched to obtain a clear aperture of .0325" square corresponding to system IFOV of 2.5 mrad. The field stop (MP19016) is constructed by cementing this aperture plate onto an aluminum supporting disk. This field stop is then mounted on a machined aluminum tube, the field stop holder (MP19010), which contains an alignment pin to ensure that the field stop is in its correct rotational orientation. The field stop is secured in this position by the field stop retainer (MP19011).

The exterior of the field stop holder is threaded to fit onto a field stop adjustment ring (MP19008). The field stop holder and adjustment ring are then assembled into the grating holder (MP19013) which is attached to the spectrometer housing (AC19001). The field stop adjustment ring allows an adjustment of ±.075" which permits the field stop to be placed precisely in the focal plane of the primary optics. A sliding pin placed between the field stop holder and the grating holder preserves the correct rotational orientation of the aperture as the adjustment ring is rotated. A locking screw is used to secure this adjustment. All of the individual assemblies which are attached to the primary thermal compensation sled, Figure 12, are made of aluminum. This is consistent with the original design of the scan head which is compensated to ensure that the aperture will remain at the primary focus throughout the total range of expected temperature variations.

2.3.1.2. COLLIMATING MIRROR. The off-axis paraboloidal mirror (MP19015) must be mounted so that the optical axis of the parent paraboloid is centered in the field stop after the primary focusing is completed. This can be accomplished by correctly aligning the rotation of the off-axis segment and also the segment's offset from the optical axis. This mount also allows a means to adjust the distance between the field stop and reference surface of the collimator.

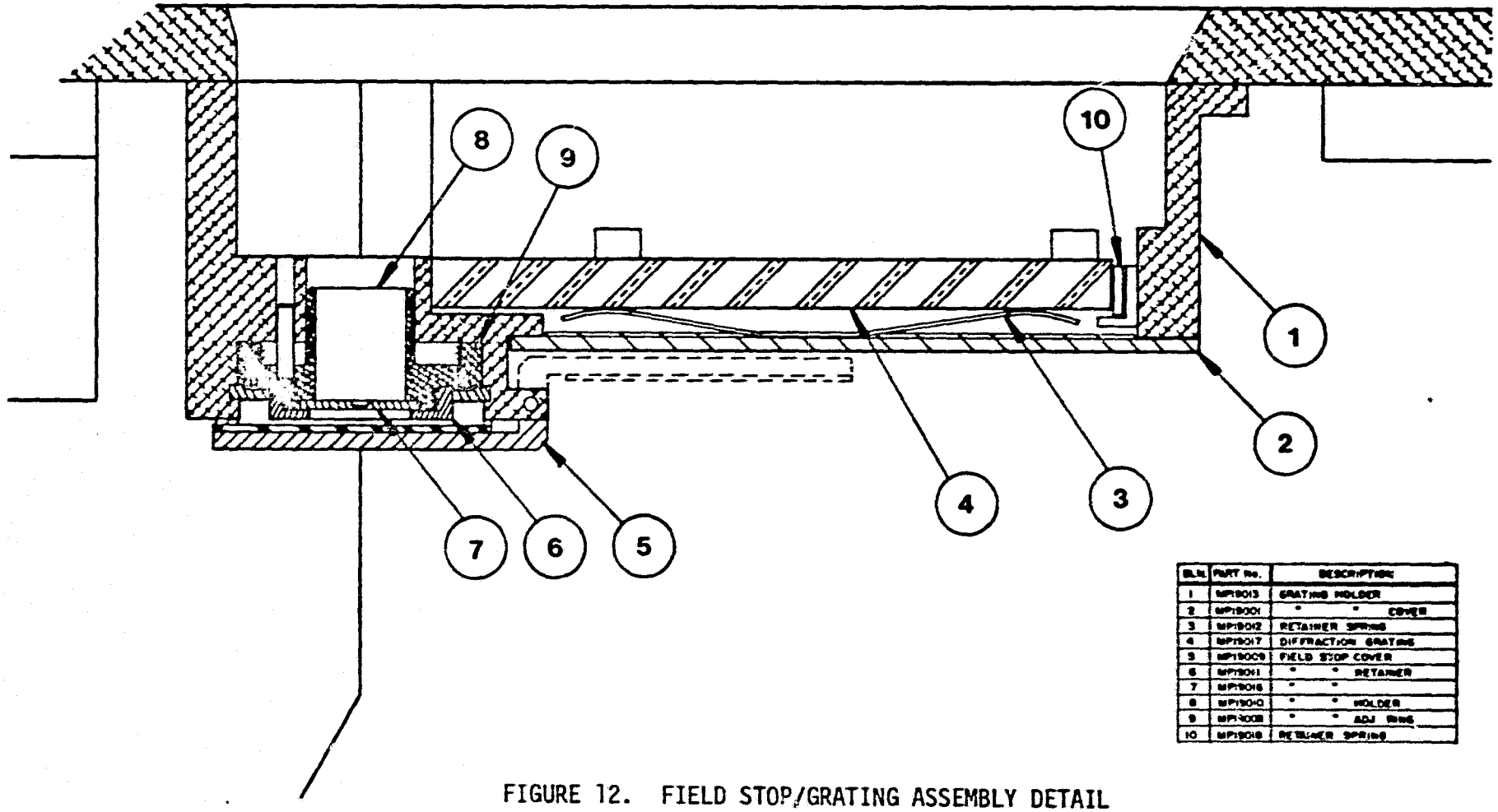

BLN.	PART No.	DESCRIPTION
1	MP19013	GRATING HOLDER
2	MP19001	" " COVER
3	MP19012	RETAINER SPRING
4	MP19017	DIFFRACTION GRATING
5	MP19009	FIELD STOP COVER
6	MP19011	" " RETAINER
7	MP19016	" "
8	MP19010	" " HOLDER
9	MP19008	" " ADJ RING
10	MP19018	RETAINER SPRING

FIGURE 12. FIELD STOP/GRATING ASSEMBLY DETAIL

The collimator is fabricated to have a flange at its base to facilitate mounting. The collimator is fitted into the off-axis paraboloid mount (MP19005) and then secured with three clamps (MP19006). These clamps are secured with screws and Belleville washers and have a thin mylar surface where they contact the mirror. The mounting plate is constructed of Invar steel which has a low thermal coefficient of expansion and, therefore, will not stress the mirror as the temperature varies.

The paraboloid mount has two holes which are located after the collimator is manufactured and in conjunction with a radial groove cut in the back surface of the mirror substrate are used to align the mirror about its rotational axis[4]. The mirror mount has two 3/16" locating dowels on its rear surface which mate with a hole and a groove in the off-axis thermal compensation slide (MP19004). This slide is made of aluminum and the groove associated with the one locating pin will allow for differential movement between the mount and slide as the temperature varies. The exact position of the locating pins are determined to thermally compensate the center of the mirror with respect to the optical axis.

The compensation slide fits into the collimator mounting base (MP19014). An alignment tab with a threaded hole provides an adjustment between the slide and the base which is locked-down with two screws after alignment. The collimator base also provides a firm support base for the paraboloid mount which is secured to the base with four screws and Belleville washers. The slotted holes in the mirror mount allow differential expansion of the assembly to take place as the ambient temperature varies, while the Belleville washers ensure that the pieces have enough compression loading between them to prevent vibration or movement in an undesired manner.

The collimator base is secured to the spectrometer housing (AC19001) using Belleville washers and slotted holes to allow

movement along the optical axis. The movement is constrained by an Invar steel bar which is attached to the off-axis paraboloid base clamp (MP19007) on one end and pinned to the spectrometer housing on the other. The clamp has slotted holes and a screw adjustment to move the paraboloid base in a controlled fashion along the direction of the optical axis. After this adjustment is made, screws are tightened to lock the clamp to the base. The exact length of the bar is calculated to provide thermal compensation for the mirror along its optical axis. The collimator assembly is shown in Figure 13.

2.3.1.3. DIFFRACTION GRATING. The grating is located in a highly congested area. The primary clear aperture, the field stop assembly, the secondary mirror holder, and the aperture cover are all in close proximity. The grating (MP19017) is mounted in the grating holder (MP19013) between four front surface mounting pads, which form the locating reference surfaces, and four spring retaining clips. This grating mount allows the grating to be safely removed permitting access to the collimator's clear aperture during an alignment procedure, if needed. The loading of the spring clips has been calculated to account for all expected g-loading and vibrational forces expected to be encountered. The grating is secured in its mount by the grating holder cover (MP19001) which is used with a gasket material to provide an environmental seal. The diffraction grating assembly is shown in Figure 12.

2.3.1.4. IMAGING LENS. The imaging lens will have a stainless steel housing (MP19022) designed to our specifications. The lens will have a mounting flange which will be fastened directly to the spectrometer housing (AC19001).

2.3.1.5. DETECTOR/DEWAR PACKAGE. The mounting of the detector/dewar package has been designed to have adjustments about three rotational axes and three translational axes as illustrated in Figure 14. Until a vendor is chosen for the detector/dewar package, the design in this area cannot be

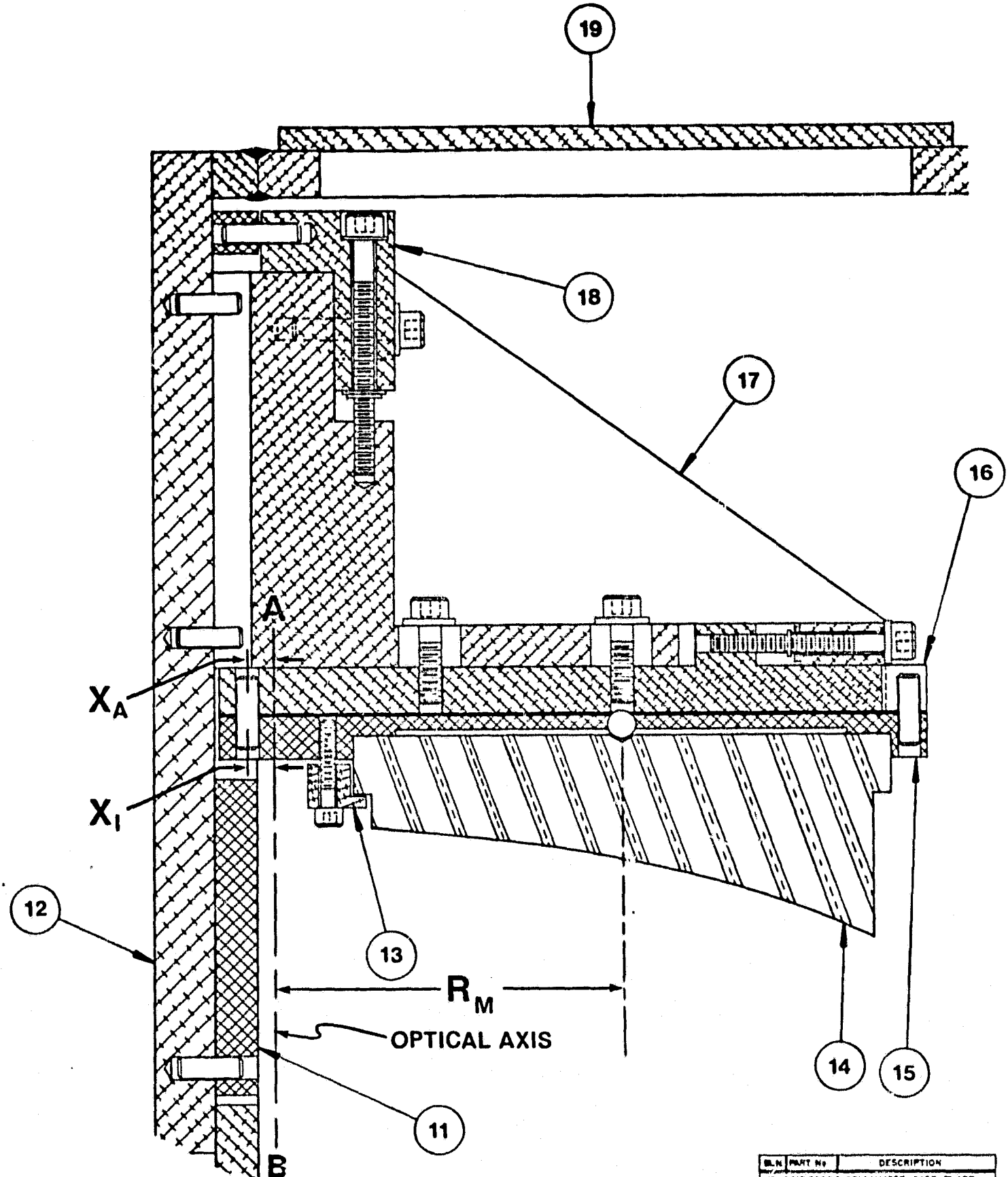

BL.N	PART No	DESCRIPTION
12	MPI9004	COLLIMATOR BASE PLATE
13	MPI9006	PARABOLOID CLAMP
14	MPI9015	OFF AXIS PARABOLOID
15	MPI9005	PARABOLOID MOUNT
16	MPI9004	THERMAL SLIDE
17	MPI9014	COLLIMATOR BASE
18	MPI9007	PARABOLOID BASE CLAMP
19	MPI9025	COLLIMATOR ACCESS COVER

FIGURE 13. COLLIMATOR ASSEMBLY DETAIL

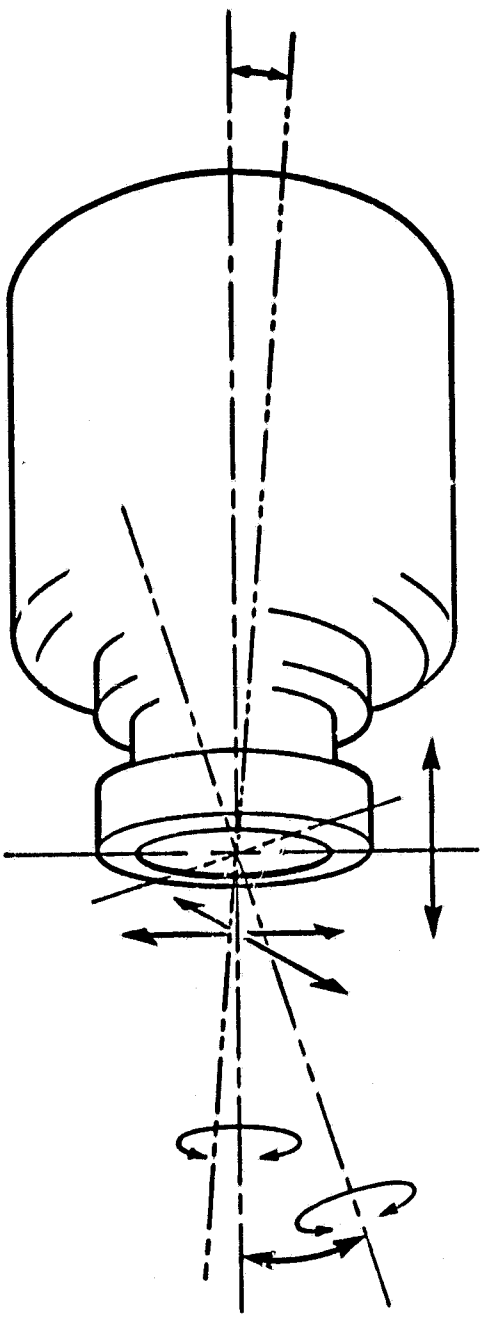

FIGURE 14. DEWAR ADJUSTMENT AXES

finalized. All of the alignment plates will be made of Invar steel; at this point, no thermal compensation is designed into the system. If the dewar is made from a 300 series stainless steel and mounted as shown in Figure 15, the expansion of the dewar will compensate for the expansion of the Invar plate. The final solution is unlikely to be this simple. When the detector/dewar package is chosen, more information about the variation in detector array position relative to the mounting surface will be known.

The roll/pitch/Z-axis adjustment will be accomplished by three adjustment screws which separate the lens mount from the roll/pitch plate (MP19003). These adjustments incorporate a thin tube mounted into a universal ball joint to effect the required motion. These adjustments will allow a .100" tilt in the plane of the detector array in two axes. The X-axis adjustment plate (MP19018) allows ±.05" of adjustment and the Y-axis adjustment plate (MP19019) allows ±.15" of adjustment. These adjustment ranges are much larger if the roll/pitch axis adjustments are not set at their limits. A rotational adjustment plate (MP19020) will allow a ±2½° fine adjustment in the rotational orientation of the detector/dewar package.

2.3.2. ALIGNMENT OF THE OPTICAL ELEMENTS

The alignment of the optical elements after the system is assembled has been given considerable thought during the design process. Although different candidate procedures have been identified, the selection of the best method will be postponed until more information is known about the problems. Laboratory testing will be done using optics from the NASA 24 channel spectrometer as well as using the actual optics purchased for TIMS.

The two areas with the most uncertainty are: 1) alignment of the collimator with respect to the field stop; and 2) placing the sensors precisely at the image plane. However, the

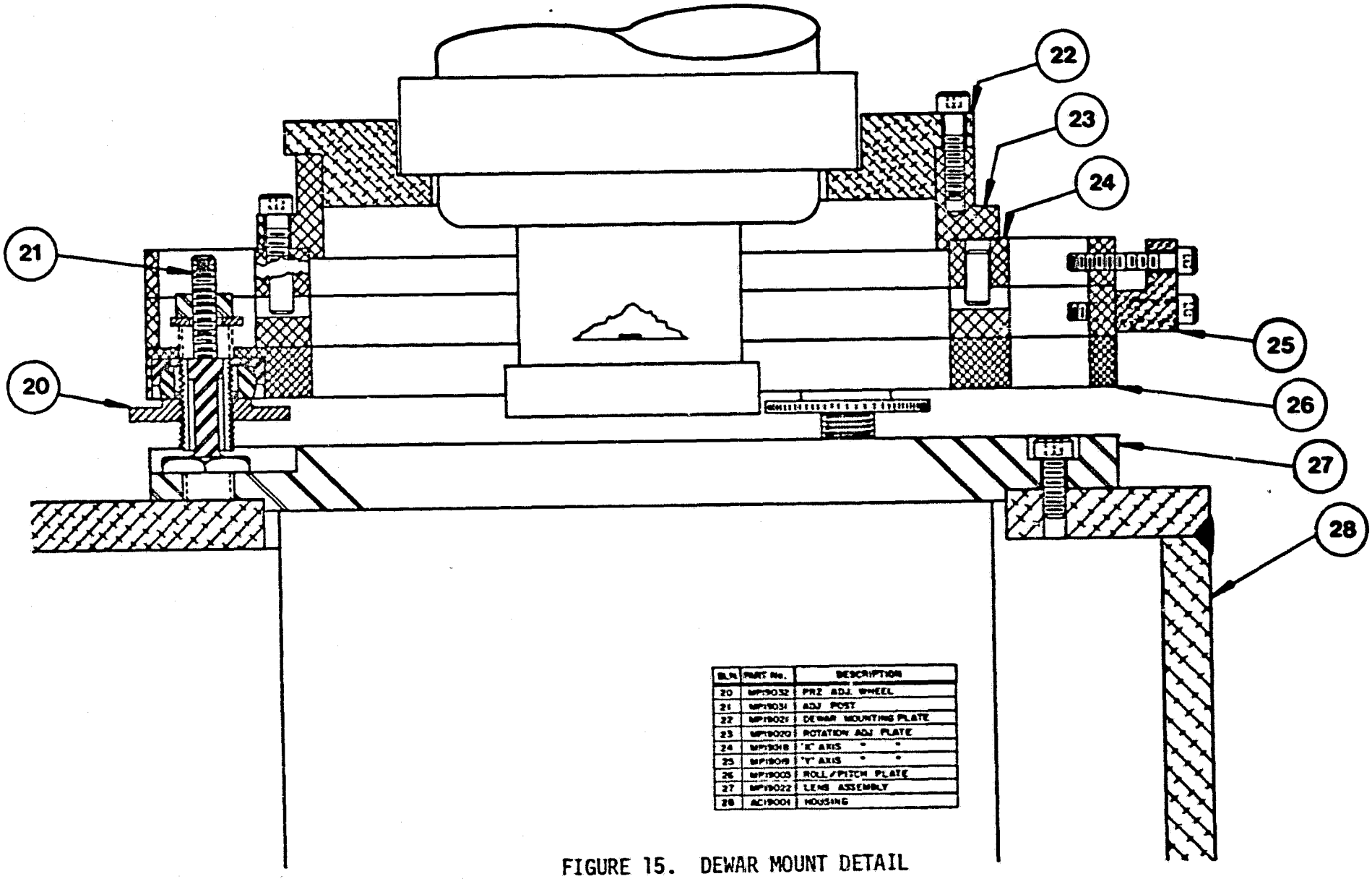

ITEM	PART No.	DESCRIPTION
20	MP19032	PRZ ADJ. WHEEL
21	MP19031	ADJ. POST
22	MP19021	DEWAR MOUNTING PLATE
23	MP19020	ROTATION ADJ. PLATE
24	MP19018	"X" AXIS " "
25	MP19019	"Y" AXIS " "
26	MP19005	ROLL/PITCH PLATE
27	MP19022	LENS ASSEMBLY
28	AC19001	HOUSING

FIGURE 15. DEWAR MOUNT DETAIL

alignment of the field stop aperture with respect to the primary paraboloid and the spectral alignment of the detector array as well as the registration of the detector array onto the image of the aperture also need to be considered.

2.3.2.1. FIELD STOP. The alignment of the field stop aperture can be accomplished by observing the electrical outputs of the detector while scanning a bar target sized at the system IFOV. This primary focus adjustment is implemented by using a special scanner wrench on the field stop adjustment ring. The contrast of the image is then inferred by observing the detector output on an oscilloscope; this should be an indication of the value of the modulation transfer function at the system resolution. Adjusting the field stop to maximize contrast will place it at the optimum focus of the primary optical system.

2.3.2.2. COLLIMATOR. Once the field stop is focused with respect to the primary optics, the whole spectrometer can be removed from the scan head and the off-axis collimating paraboloid aligned. The difficulty with aligning the off-axis paraboloid is that the location of its vertex is not within the perimeter of the segment and its location, therefore, is unknown. A procedure for finding this vertex after the segment has been cored out of the parent paraboloid has been described by Mitchell Ruda of Talandix Research Corporation[4]. A portion of this technique will be used. Specifically, a method of locating the parent vertex will be employed which requires that various operations and measurements be performed by the paraboloid vendor before and after removal of the segment from the parent paraboloid.

As shown in Figure 16, a V groove will be machined in the back surface of the parent paraboloid at a radial distance from the vertex. The radius of this groove should be approximately equal to the distance to the center of the cored section from the parent vertex. The exact radius is not important;

however, it must be measured accurately after the groove is cut and before the section is cored. When this measurement is known, two holes will be located in a paraboloid mount (MP19005) at the exact radial distance from the desired portion of the parent vertex. These holes will be temporarily filled with spring loaded steel balls that will fit into the V groove on the paraboloid only when it is oriented correctly. The correct rotational orientation of the paraboloid will then be defined and the mirror will be clamped in place. The tilt of the section will be determined by closely controlling the manufacture of the mirror and the other assemblies in the spectrometer.

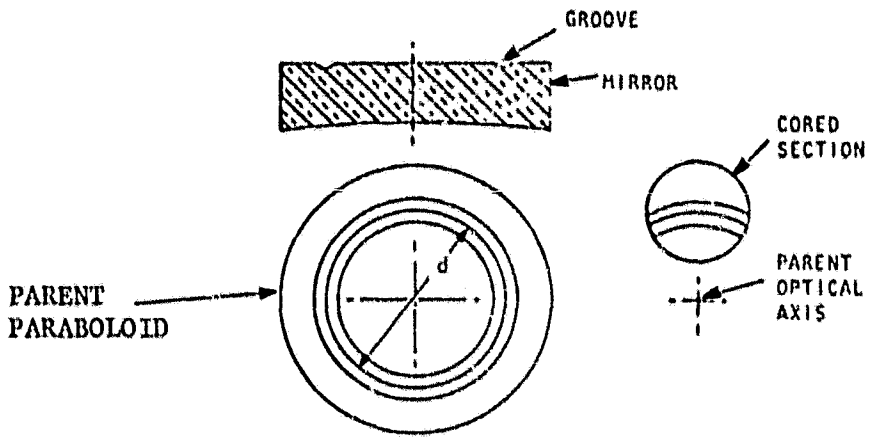

FIGURE 16. OFF-AXIS PARABOLA V GROOVE ILLUSTRATION

The mirror also needs to be located with respect to the field stop. The parameter of importance here is that the vertex of the parent mirror (i.e., the optical axis) be positioned on a line intersecting the center of the field stop aperture and forming the proper angle of 25° with a line normal to the grating surface. The best method to properly locate the vertex of the paraboloid on this line is unknown at this time. Some of the candidate methods are: 1) Illuminate the parabola with an expanded visible laser beam which

has been carefully aligned to 25° with respect to the line normal to the grating surface. This can be accomplished by removing the grating and mounting the laser fixture to the grating mounting pads. The paraboloid adjustment in the radial direction is then made while observing the focused laser beam in the field stop aperture with an alignment telescope; and 2) Measure the distances along known references on the spectrometer and set the paraboloid vertex on this line as determined by the information given by the paraboloid vendor and the mechanical design details. The adjustment of the paraboloid focus can be made using either of these methods.

2.3.2.3. DIFFRACTION GRATING. The diffraction grating location is fixed and no alignment is needed.

2.3.2.4. IMAGING LENS. The location of the imaging lens is fixed and no alignment is needed.

2.3.2.5. DETECTOR/DEWAR ASSEMBLY. This assembly is likely to be the most difficult to align. The procedures for aligning the other components, while not simple, have the potential advantage of using visible light and, therefore, the human eye to help the process. Beyond the imaging lens, only infrared energy is available (or useful) to accomplish the alignment; therefore, the sensors themselves must be used. The technique of aligning, focusing, and spectrally calibrating the detector array is likely to involve several iterative steps; the sequence of which will be determined experimentally.

Spectral alignment and initial array focus can be achieved by combinations of field stops, optical filters, and mirror(s) at the grating plane. Replacing the grating with a mirror produces an undispersed image of the field stop at the image plane. By altering the angle of this mirror with respect to the collimator, the image can be positioned to correspond to any equivalent spectral band at the image plane. With the normal square field stop in place and the mirror positioned to illuminate one of the square detector elements, an

approximate focus and spectral calibration may be found by moving the array until the signal from this element is maximized. A more accurate spectral alignment would involve refinement of this technique such as:

1. Replacing the square field stop with a slit 0.004" x 0.032" oriented to place the smaller dimension in the dispersing direction at the image plane.
2. Placing a mirror at the grating plane, properly angled to place the field stop image at the 10.2 μm wavelength position, which is the center of the central gap in the detector array.
3. By observing the outputs of bands 4 and 5, the array may be accurately positioned so that all of the energy from the field stop slit falls onto the inactive area between these elements (image size will be ∿0.002" x 0.015").

For greater accuracy, chromatic aberrations from the imaging lens may be reduced by limiting the wavelength at the image plane with a bandpass filter placed ahead of the lens.

The successful method of alignment, focusing, and calibration will probably involve refinements and iterations of these techniques.

2.3.3. ENVIRONMENTAL PROTECTION

The spectrometer described in this report will be operated in a high altitude aircraft in an unpressurized environment. During ascent and descent, large variations in pressure and temperature will occur. One of the likely occurrences will be an aircraft operation at high altitudes where the scanner will be subject to low pressures and low temperatures. Then, an immediate descent to an airport will return the scanner to sea level pressure and warm humid air. Under these conditions,

it is almost certain that the scanner temperature will be below the dew point of the air and, therefore, condensation will occur. This condensation can have potentially harmful effects on the system performance and reliability.

The mirrors are coated with an aluminum surface and then overcoated with a silicon monoxide protective layer. The lens elements have anti-reflective coatings on them. These coatings are susceptible to temporary and permanent damage from moisture. This will be especially true of the grating since any cleaning of its surface is likely to cause damage. Any contamination of the optical surfaces by hydrocarbons will be detrimental to the intended use of the scanner because of their selective spectral absorption bands. Therefore, consideration has been given to methods of preventing such damage to the system.

The most obvious method would be to completely seal the system from the environment. The optical entrance apertures are obvious places to consider. Sealing the primary entrance aperture would require a carefully ground and corrected germanium window at least 7.5" x 21" in size and thick enough to withstand a large pressure differential. Sealing the entrance aperture to the spectrometer would require a smaller window; however, its location in the focal plane of the primary optics would be unacceptable. Neither one of these methods appears to be practical; therefore, the solution that we have adopted is to purge the spectrometer during aircraft descent and to seal the unit when it is not operating.

The spectrometer is, therefore, designed to be a sealed unit with two openings. One opening is, of course, the field stop aperture. This opening has a pivoting cover with a sealing gasket and is electrically operated. This cover would normally be in place whenever the scanner is not being operated. The other opening is a connector for 1/4" diameter Tygon® tubing.

At this point the exact operation of the system is undefined. The tubing could be connected to an expendable source of dry nitrogen gas or it may be connected to a filter and desiccant. The spectrometer could also be fitted with a differential pressure sensor and two temperature sensors. One temperature sensor would be mounted internally to the spectrometer in a location with a high thermal mass. The other sensor would have very low thermal mass and sense the ambient temperature. The pressure sensor could be used to detect any small negative pressure differentials between the inside of the spectrometer and the ambient and then activate the nitrogen gas purge. The temperature sensors would detect when the spectrometer temperature has reached within 1°C of ambient and turnoff the nitrogen and close the field stop aperture cover.

Alternately, a manual system could be employed which would require the operator to close the field stop aperture at operating altitude before descent. Then the spectrometer would become filled with the atmosphere through the filter and desiccant. Some combination of these ideas could be implemented. However, we have provided some means to accomplish the protection of the spectrometer optics even though the actual implementation has not been completed.

These are some of the ideas presently being considered and no firm decision has been made.

2.3.4. THERMAL COMPENSATION

During the design of this spectrometer, special consideration had to be given to shifts in alignment which could be caused by changes in the ambient temperature. Two approaches were considered: 1) provide a stable thermal environment for the whole spectrometer; or 2) thermally compensate for movements encountered by mechanical means.

The first approach simplifies the spectrometer design task, but places a significant burden on the aircraft support

system. Because of this and because the primary telescope design is already compensated, it was decided to also compensate the spectrometer design. The basic approach, which will be covered in detail in the following sections, is to utilize the difference in linear coefficients of thermal expansion of the differing materials. The selected materials were aluminum (6061T6) and Invar, a high nickel alloy steel. The coefficients of expansion of these materials vary from batch to batch by ±15%. It will be shown that these variations have a negligible effect on the design. Because the Invar steel is difficult to machine, it is used in the design only where its thermal characteristics are essential. In the subsequent sections, the values of the coefficients of Invar and aluminum will be assumed to be:

$$\text{Aluminum: } \alpha_A = 21.7\ (10^{-6})\ \text{in. in.}^{-1}\ {}^{\circ}\text{K}^{-1}$$

$$\text{Invar: } \alpha_A = 1.35\ (10^{-6})\ \text{in. in.}^{-1}\ {}^{\circ}\text{K}^{-1}$$

The concepts implemented in this thermal compensation method have been used successfully by Daedalus and proven in practice with the AADS1280 scanner system delivered to NASA in November, 1979. The AADS1280 scanner system has an IFOV of 0.54 mrad and the tolerances on the position of the optical components over temperature are of the same magnitude as those needed in the TIMS spectrometer.

2.3.4.1. FIELD STOP. The field stop is mounted in an all-aluminum holder which is attached to the thermal compensation sled of the primary optics. The scan head design allows differential movement of the primary paraboloid, the compensation sled, and the secondary mirror mount. These movements will ensure that the field stop aperture remains in the focal plane of the primary optical system. The compensation sled is, in fact, part of the spectrometer housing thereby ensuring that thermal compensation of the spectrometer can be effected independently of the primary compensation.

2.3.4.2. COLLIMATOR LATERAL COMPENSATION. The collimator is constructed from Zerodur®, a glass-like ceramic with excellent dimensional characteristics. The thermal coefficient of linear expansion is extremely small, α_Z = .08 (10^{-6}) in. in.$^{-1}$ °K^{-1}. This low coefficient of expansion means that it will maintain its proper curvature over the temperature range and will also create a minimum amount of stress in its Invar mount.

The Invar collimator mounting plate is fastened to an aluminum sliding compensation bar and supported by the paraboloid base. Each of these pieces is designed with slotted sections, locating pins, and fastened together using slotted holes and Belleville washers with the fasteners. This arrangement provides the necessary thermal compensation to keep the mirror in its proper position relative to its optical axis. Consider the assembly as shown in Figure 13. Line AB, the optical axis of the full (parent) paraboloid, is the reference plane for the assembly. The center of the collimator is required to remain at a constant distance from this optical axis. This distance is referred to as R_M and is calculated to be 2.837".

If the collimator were mounted using aluminum materials, a shift in the location of the center of the mirror from the axis, over an 80°K change in temperature, would be:

$$R_M \alpha_A \Delta T = 2.837 \cdot 21.7 \cdot 10^{-6} \cdot 80 = .005"$$

The collimator mounting plate cannot be constructed from aluminum because the large difference between α_A and α_Z would produce stresses that would distort the optical surface and possibly crack the substrate. If the collimator mounting plate is made from Invar, pinned on the optical axis and maintains a sliding interface along the remainder of its surface, the shift can be reduced to:

$$R_M \alpha_A \Delta T = 2.837 \cdot 1.35 \cdot 10^{-6} \cdot 80 = .0003".$$

This magnitude of shift would be acceptable; however, once the locating pin and the sliding mount are designed, a slight change in the pin location can result in a theoretical zero shift in mirror position as a function of temperature.

Referring to Figure 13, the aluminum parabola bar (MP19004) is solidly attached to the aluminum base (MP19014). The Invar mirror mount (MP19005) is fastened to the slide at the pin location on line CD displaced at a distance X from the optical axis AB. The center of the mirror is, therefore, located at a distance Y from the optical axis as shown in Equation (1).

$$Y = - X_A + X_I + R_M. \tag{1}$$

We can now consider the initial condition to some temperature (+25° for instance); at this temperature, $X_A = X_I$ and $R_M = 2.837$. Now if we examine the partial differential of Y with respect to temperature, we obtain Equation (2):

$$\frac{\partial Y}{\partial T} = - X_A \alpha_A + X_I \alpha_I + R_M \alpha_I. \tag{2}$$

If we consider all other variables to be constant, then the change in the mirror position is represented by Equation (3):

$$\Delta Y = - X_A \alpha_A \Delta T + X_I \alpha_I \Delta T + R_M \alpha_I \Delta T. \tag{3}$$

If we now set $\partial Y/\partial T$ to be zero and solve for the distance X, using Equation (2), we find:

$$X = \frac{R_M \alpha_I}{(\alpha_A - \alpha_I)} = \frac{2.837(1.35) \cdot 10^{-6}}{(21.7-1.35) \cdot 10^{-6}} = .189".$$

If we set the distance X as .189", the center of the mirror will always remain 2.837" from the optical axis if it can be assumed that: 1) the coefficients of expansion are linear over the temperature range; 2) the coefficients used in the calculation represent the actual materials used; 3) the pin location

is as calculated; and 4) the pieces slide freely with zero stress buildup. In reality, we can say that none of these assumptions are true; but we can examine the sensitivity to these sources of error by taking the partial derivative of Equation (3) with respect to the variables of interest. For example, the manufacturer's data sheets for the Invar steel indicate that the coefficient α_I can vary by ±15% over the temperature range of -50 to +100°C. The partial derivative of Equation (3) with respect to α_I is:

$$\frac{\partial \Delta Y}{\partial \alpha_I} = X_I \Delta T + R_M \Delta T.$$

Therefore, a variation of +15% in α_I from 1.35 to 1.55 would yield a change in the perfect compensation ($\Delta Y = 0$) equal to $X_I \Delta T \Delta\alpha_I + R_M \Delta T \Delta\alpha_I$. This can be evaluated over an 80°K temperature change to be only (2.837 + .189")(80°K)(.2 in. in.$^{-1}$ °K^{-1} = .000048". In a like manner, the sensitivities to pin locations and non-linear coefficients can be shown to be negligible. The stress buildup and deflection of the pieces due to the coefficient of sliding friction has not been evaluated; but is likely to be small because all sliding parts will be Teflon® coated to minimize frictional forces.

2.3.4.3. COLLIMATOR AXIAL COMPENSATION. The rationale for and the design of the thermal compensation used to maintain the collimator's position along the optical axis is similar to that discussed in Section 2.3.4.2. The back of the paraboloid base (MP19015), line EF, serves as a reference plane as shown in Figure 17. The distance between this reference plane (line EF) and the field stop should be kept constant as a function of temperature. An equation for this distance can be written and is presented as Equation (4):

$$f = \text{distance from base to field stop} = Z_A + Q_I - W_A \qquad (4)$$

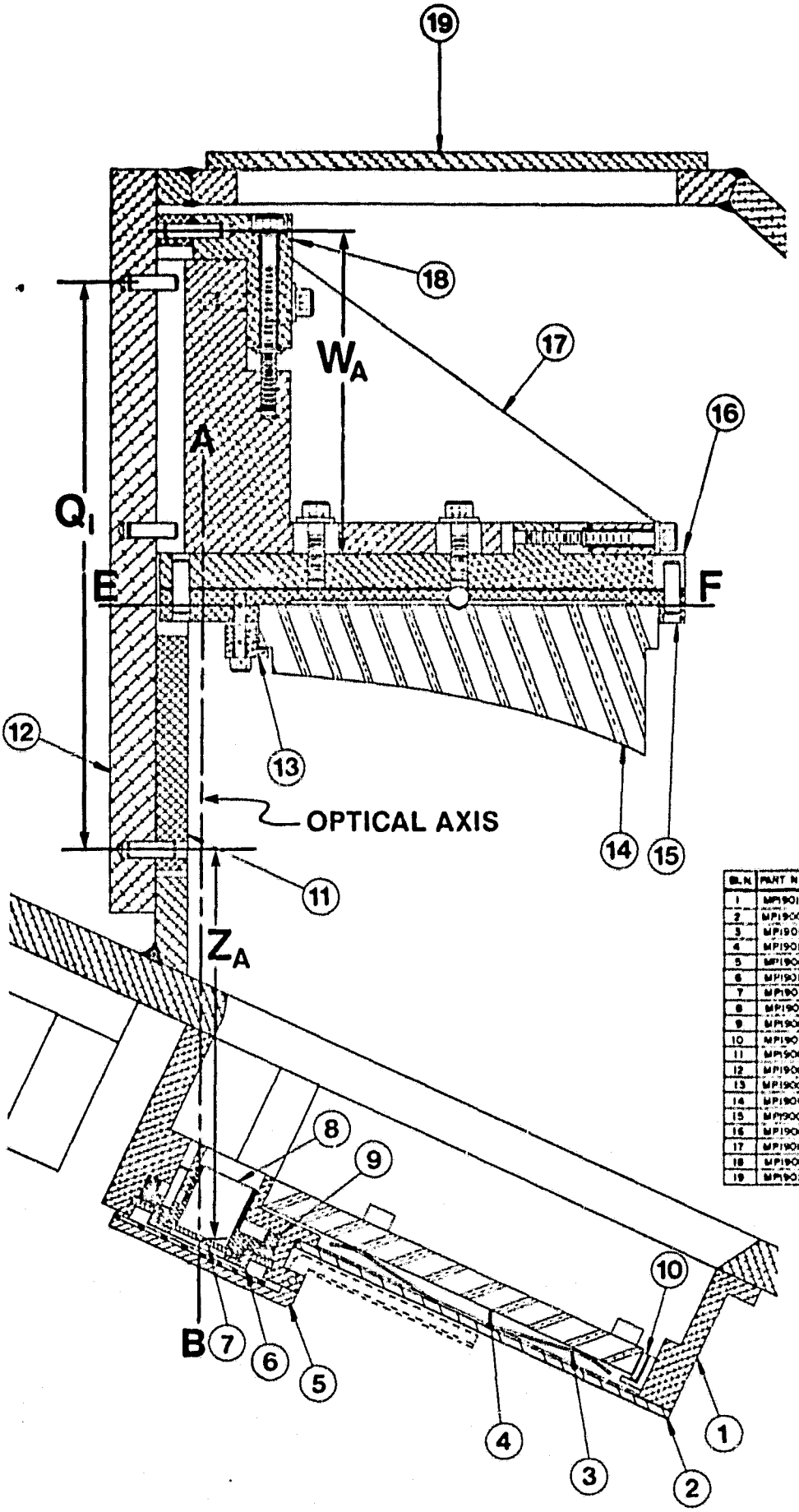

BL.N	PART No	DESCRIPTION
1	MP19013	GRATING HOLDER
2	MP19001	" " COVER
3	MP19012	RETAINER SPRING
4	MP19017	DIFFRACTION GRATING
5	MP19009	FIELD STOP COVER
6	MP19011	" " RETAINER
7	MP19016	" "
8	MP19010	" " HOLDER
9	MP19008	" " ADJ RING
10	MP19018	RETAINER SPRING
11	MP19002	THERMAL COMPENSATION BAR
12	MP19004	COLLIMATOR BASE PLATE
13	MP19006	PARABOLOID CLAMP
14	MP19015	OFF AXIS PARABOLOID
15	MP19005	PARABOLOID MOUNT
16	MP19004	" THERMAL SLIDE
17	MP19014	COLLIMATOR BASE
18	MP19007	PARABOLOID BASE CLAMP
19	MP19023	COLLIMATOR ACCESS COVER

FIGURE 17. COLLIMATOR THERMAL COMPENSATION DETAIL

When this equation is differentiated with respect to temperature and evaluated assuming all variables are constant, then:

$$\Delta f = (Z_A - W_A)\ \alpha_A\ \Delta T + Q_I\ \alpha_I\ \Delta T. \qquad (5)$$

By setting Δf equal to zero and knowing the focal plane of the mirror, the distances Z_A and W_A, Equation (5) can be solved to find the distance Q_I. Once these pin locations on the Invar bar are determined, the assembly will be perfectly thermally compensated in axial position within the same limitations discussed in Section 2.3.4.2.

2.3.4.4. DIFFRACTION GRATING. The diffraction grating is placed in the optical system so that it receives the collimated energy from the paraboloid. Therefore, the distance between the paraboloid and the grating can be allowed to vary without adverse effects. The angle between the collimated energy and the normal to the surface of the grating is important. This angle is determined by the precise machining of the supporting structure. Since all the materials that determine the angle are constructed of the same material (aluminum), the angles will not change as a function of temperature.

2.3.4.5. IMAGING LENS. The imaging lens will be purchased as a complete assembly and will be internally compensated with respect to focal changes over the required temperature range. As with the grating, the lens input is a collimated beam so that the distance between it and the grating is not critical. The angle between the lens and the grating is critical, but will remain constant over the temperature range since all of the components determining this angle are fabricated from the same type of aluminum.

2.3.4.6. DETECTOR/DEWAR PACKAGE. The mounting of the detector/dewar package with respect to the imaging lens is very critical to the system performance. The detector plane is at the focus of a fast (f.8) lens and because of the large cone angle of the rays, a focal shift of greater than ±.0005" would be

excessive (reference Section 2.2.4). As stated in Section 2.3.4.5, the lens focal plane will be thermally compensated with respect to a reference point on the lens cell. The detector/dewar package will be a stainless steel vacuum dewar with a mounting ring which serves as a reference (see Figure 15). At this point the thermal characteristics of the dewar are unknown. The specification for the detector/dewar package requires that the vendor furnish us with the required information on the thermal properties of the package as a part of the contract. We have specified that the dewar be fitted with a pressure relief valve to maintain a constant pressure; hence, a constant temperature within the dewar. However, dimensions of the outside jacket of the dewar will vary with ambient temperature. The internal support to the cold finger may also vary in length since it will see a changing thermal gradient across its length. We suspect that parts of the detector/dewar mount will need to be redesigned after we receive the necessary information from the detector vendor.

2.4. SENSITIVITY ANALYSIS

An infrared imaging device that uses a photon detector records a signal that is proportional to the number of photons per unit time. In the absence of a signal, the system is said to record only noise. An AC system will record the fluctuations about the average background radiance. The targets currently of interest will have a change in radiance from both temperature and emissivity. The targets will be larger than the IFOV and the recorded signal will correspond to the radiance. Several expressions describe the ability of an infrared system to sense a change in radiant power. We will use only signal to noise ratio (SNR), and noise equivalent temperature difference (NETD).

High performance photoconductive MCT detectors have a quantum efficiency of near unity. The detector is capable of background limited performance. A standard expression to

calculate SNR uses quantum efficiency, cutoff wavelength, and incident background flux. The detector specification requires D* to be equal to or greater than a minimum value for each spectral channel. At this time the detector cutoff wavelengths and the cold shield geometry cannot be defined. Lacking this information, the SNR expression is derived based on known information and conservative estimates of optical throughput.

An expression using power in place of photon flux allows direct calculation of SNR without the need of detector cutoff wavelength. The expression may be written as:

$$SNR = \tau_o \tau_a \pi \sin^2 A \sqrt{\frac{A_d}{\Delta f}} \left[\int_{\lambda_1}^{\lambda_2} \tau(\lambda) G(\lambda) D^*(\lambda) \frac{\partial L}{\partial T}(\lambda) d\lambda \right] \Delta T$$

where

$\sin A = 1/2\ f/N$ for an aplanatic lens or one that is nearly so

τ_o = optical transmission

τ_a = atmospheric transmission

A_d = detector area

Δf = electrical noise bandwidth

$\tau(\lambda)$ = cold filter transmission

$G(\lambda)$ = grating efficiency

$D^*(\lambda)$ = detector figure of merit

$\frac{\partial L}{\partial T}(\lambda)$ = radiance temperature contrast

Detector D* measurements are a function of incident background photon flux density and viewing geometry. Given the background temperature during this measurement, an equivalent D* can be calculated for a different background temperature. Assuming the detector view geometry is filled by either background, the calculation can proceed as follows:

$$D(T2) = D(T1) \sqrt{PB(T1)/PB(T2)}\ .$$

The PB(T) terms represent photon sterance, the D(T) terms represent D*, and T is the temperature in Kelvin. This ratio expression will be used to calculate D* for both scanner housing background temperatures different than 300K and cold filter background blocking. It will be assumed that all background surfaces, including the lens, have unit emissivity. As a result of this last assumption, calculated D* values will be lower than actual system performance may indicate. The reason for taking this approach is the lack of firm geometric information about the cold shield and dewar. Without knowing the cold shield geometry, it is impossible to calculate the detector view angle along the array length.

Four values of photon sterance are listed below and will be used to calculate D*:

$$Lq\ (.1,14,300) = 3.69 \times 10 \text{ photons } sec^{-1}\ cm^{-2}\ sr^{-1}$$
$$Lq\ (.1,14,343) = 7.02 \times 10 \text{ photons } sec^{-1}\ cm^{-2}\ sr^{-1}$$
$$Lq\ (8,14,300) = 3.01 \times 10 \text{ photons } sec^{-1}\ cm^{-2}\ sr^{-1}$$
$$Lq\ (8,14,343) = 5.30 \times 10 \text{ photons } sec^{-1}\ cm^{-2}\ sr^{-1}$$

The parenthetical numbers indicate short wavelength, long wavelength, and Kelvin temperature.

All of the wavelength dependent terms will be evaluated for each spectral band and the integral will be approximated by forming an average product for each band. Figure 18 shows the transmission characteristic of a typical wide bandpass filter. The selected average transmission is shown in Table 9. The grating efficiency of Figure 4 and D* of the detector specification are also tabularized. The remaining wavelength dependent term, radiance contrast, was evaluated by integration over each wavelength band. This assumes that the other terms, or their averages, are constant over the integration interval.

Optical transmission can be evaluated on a per surface basis. Starting with the scanner, an average transmission factor is calculated by dividing the active area by the total

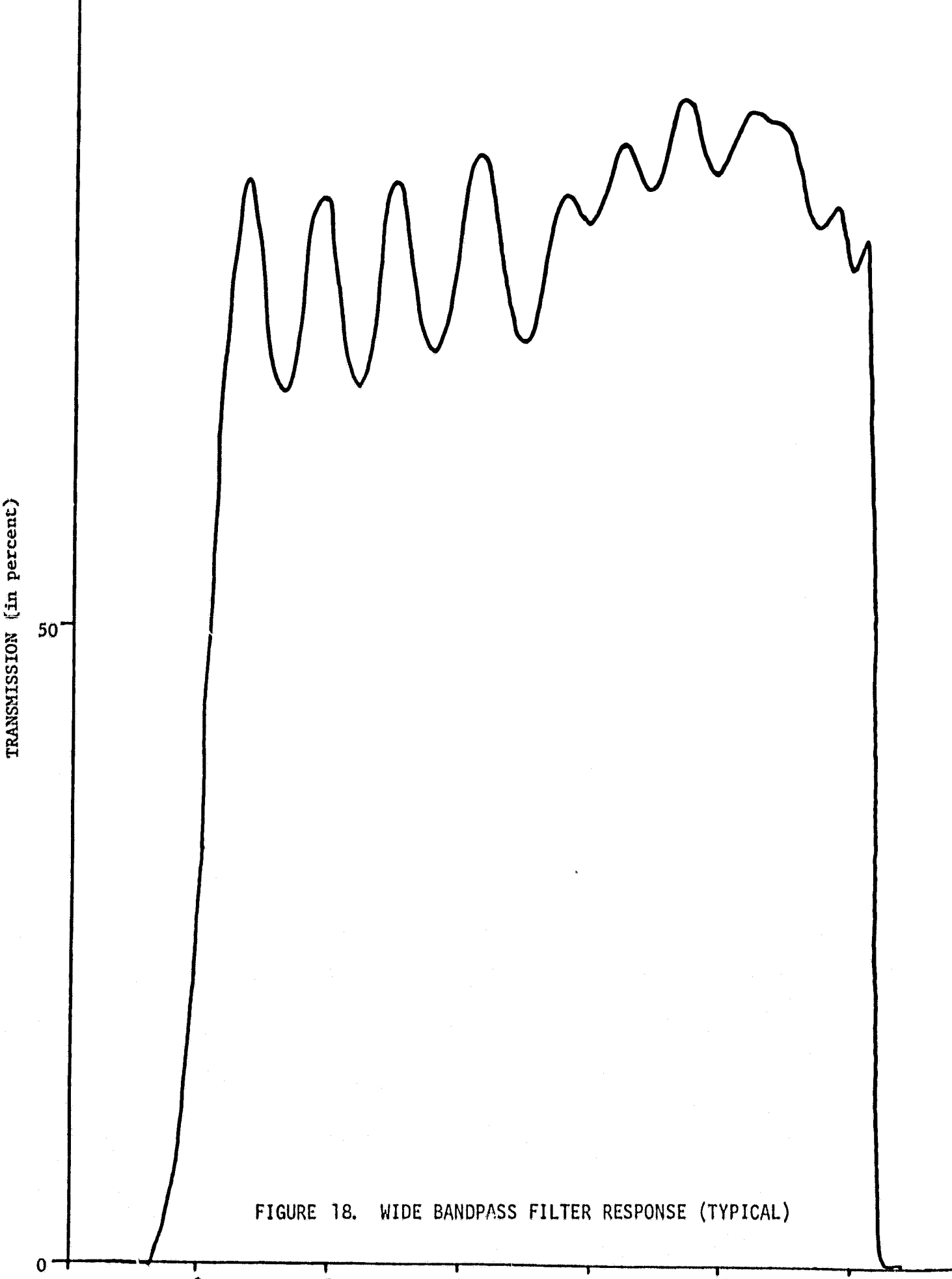

FIGURE 18. WIDE BANDPASS FILTER RESPONSE (TYPICAL)

TABLE 9. SENSITIVITY ANALYSIS

ASSUMPTIONS:

Target Temperature	= 300K
Telescope Transmission	= (active area/total area) = (36/44.2) = 0.815
Mirror Reflectivity	= 0.95 per surface, 4 surfaces = 0.81
Lense Transmission	= 0.92 per element, 3 elements = 0.78
Electronic Noise Bandwidth	= 32 KHz (25 scans/second)

$\tau_o \tau_a \pi \sin^2 A = 0.6342$

Wavelength	8.4	8.8	9.2	9.8	10.7	11.7
Bandwidth	0.4	0.4	0.4	0.8	1.0	1.0
W cm^{-2} sr^{-1} x 10^6	7.23	7.11	6.91	13.07	14.67	12.74
D x 10^{-10}*	2.7	2.8	2.9	1.8	1.9	1.8
Detector cm^2 x 10^3	1.40	1.36	1.40	2.66	3.39	3.39
Filter Tx	0.75	0.75	0.70	0.78	0.80	0.82
*Efficiency**	0.87	0.88	0.90	0.87	0.80	0.71
SNR per °K	16.9	17.2	16.8	29.2	36.8	27.6
NETD (S/N) = 1	0.06	0.06	0.06	0.03	0.03	0.04
NETD (0.1,14,343)	0.08	0.08	0.08	0.05	0.04	0.05
NETD (8,14,200)	0.05	0.05	0.05	0.03	0.02	0.03
NETD (8,14,343)	0.07	0.07	0.07	0.04	0.03	0.04

NOTE: Parameters for NETD are: 1) cut-on wavelength; 2) cut-off wavelength; and 3) scanner temperature

*Grating Efficiency

area (36/44.18) = 0.81. Typical mirror reflectance is 0.95; we have four surfaces: scan mirror, primary, folding flat, and collimator. The result is $0.95^4 = 0.81$. Next is the three element A/R coated germanium lens. Each element will have a transmission greater than 0.92 or a total transmission of $0.92^3 = 0.78$. The total optical transmission is 0.81 x 0.81 x 0.78 = 0.5168. The dewar window is not considered here since it is included in the D* specification.

The detector array sees a f/0.8 beam on each element.

A totally transparent atmosphere is assumed.

Table 9 shows the results of calculations based on these assumptions. Energy losses from image degradation of 50% would not exceed the system sensitivity requirement of 0.3°K per channel. These calculations show adequate sensitivity to meet or exceed all contract specifications.

The wavelength selected for peak grating efficiency is a compromise between high efficiency in the 0.4 μm wide spectral bands and sufficient energy at 12.2 μm. A good balance is found if the grating is blazed for 9.1 μm. Calculation of blaze angle for the 12 groove/mm grating for incident angle = 25° is:

$$9.1 \times .012 - \sin(25) = \sin(D); \quad D = -18.265°.$$

The negative sign indicates that the incident and diffracted beams are on opposite sides of the grating normal.

$$\text{Blaze Angle} = [25 + (-18.265)]/2 = 3.367°.$$

A tolerance of ±0.1° is acceptable.

2.5. SYSTEM OVERVIEW

A complete Thermal Infrared Multispectral Scanner system (TIMS) contains the major components shown in Figure 19. Of these components this study concentrates on the spectrometer and the scan head. An overview of the remaining components will help to visualize the complete system.

The bulk of video signal processing is performed by the digitizer. It accepts the six analog data signals from the spectrometer preamplifiers, converts them to a digital representation, combines them with significant auxiliary data, and encodes them into a format suitable for use with high density tape recording. Functions within the digitizer are controlled by timing signals originating at the scan motor optical encoder and processed by the video synchronizer within the operator console. The encoder signal synchronizes all video sampling and other critical timing sequences.

The operator console also contains function controls and a monitor oscilloscope. Circuits that adjust the speed and control the stability of the scan motor are contained in the controller and power distributor. Also within this unit is circuitry for monitoring and controlling the thermal reference sources on the scan head. Aircraft roll stabilization of the data is performed in the digitizer using a signal generated by the gyro and conditioned in the operator console.

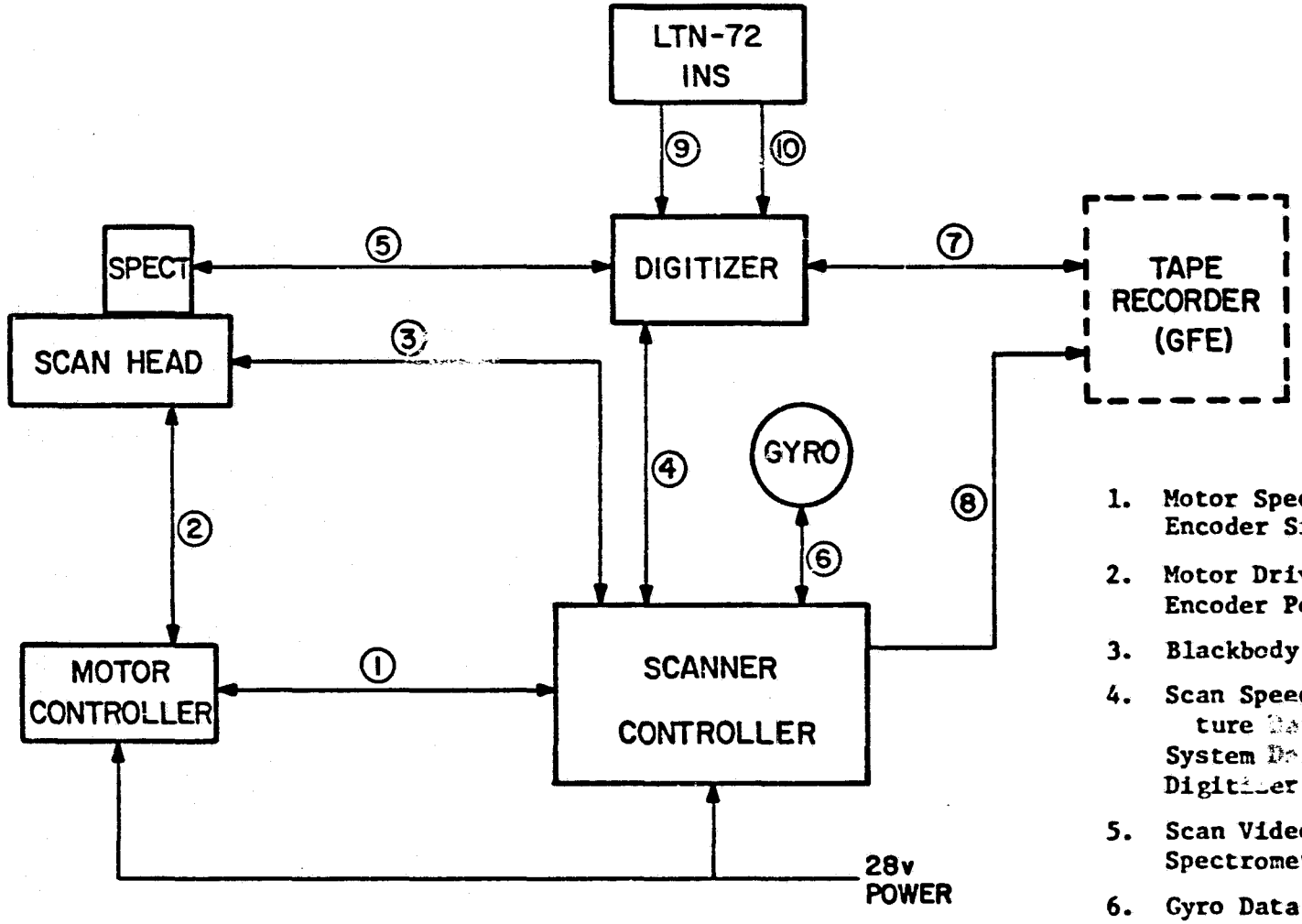

1. Motor Speed Control Signal & Encoder Signals
2. Motor Drive Power Encoder Power & Signals
3. Blackbody Data & Power
4. Scan Speed & Reference Temperature Data System Data & Monitor Video Digitizer Power
5. Scan Video Data Spectrometer Power
6. Gyro Data Gyro Power
7. Record Data Reproduce Data
8. Power & Tape Speed Reference
9. Analog Synchro Data
10. ARINC BCD Data Bus

FIGURE 19. BLOCK DIAGRAM-TIMS SYSTEM

3
CONCLUSIONS

This study concludes that a multispectral scanner system operating in the thermal infrared wavelength region is feasible and practical, utilizing the Daedalus Enterprises, Inc. ABDE116 scan head design. The study provides the following answers to questions or tasks outlined in the Statement of Work.

1. The use of a cold stop placed at a focal point in the spectrometer will not improve the system performance (Section 2.2.6).

2. The requirements for the collimator, grating, array lens, and MCT array have been analyzed and specifications written for each (Section 5).

3. The study has considered the following parameters: a) the optical layout (Section 2.2.3); b) optical surface quality (Sections 2.2.1 and 2.2.4); and c) optical positioning tolerances and their affect on NETD, channel crosstalk and spectral purity (Section 2.3.4).

4. The study has investigated the trade-offs in the specifications for the sensor array (Section 2.2.5) and generated vendor specifications for a 6-element photoconductive MCT array/dewar assembly. This array is the heart of the spectrometer and its performance will determine the final system sensitivity performance. The specifications generated are stringent but are considered feasible by several detector vendors without pushing the state of the art.

5. The study concluded that temperature compensation is required in the design of the mechanical assembly and within the imaging lens assembly itself in order to maintain the desired performance (Section 2.2.4); this was included in the design.

6. The method of mounting all optical elements was analyzed. Mounting schemes were designed that consider both

performance criteria and methods of achieving alignment (Sections 2.3.1 and 2.3.2). Many of the mechanical components will require precision machining to close tolerances by a skilled craftsman to meet the system performance requirements. Achieving this precision in the manufacturing process permits minimizing the number of adjustments and, therefore, produces a more stable assembly. The array dewar should be metal for thermal compensation design; it should have a pressure relief valve on the LN_2 chamber. The array should be cold shielded to the extent that the optic system permits.

7. The system can be rapidly converted to a 6-band 1-2.5 μm scanner, or other wavelength bands for which a suitable spectrometer can be designed (Section 2.2.7). The design of other spectrometers was not investigated.

8. The design of the ABDE116 scan head has been successfully modified to accommodate the IR spectrometer and thermal reference sources (Section 2.1.2). The changes required do not disturb the basic design and thermal compensation of the head.

9. A theoretical sensitivity analysis (NETD) was performed on the system, considering all significant component parameters; its result indicates the system will surpass a sensitivity goal of NETD $\leq$ 0.3°C in each band by a considerable margin (Section 2.4). The magnitude by which this calculated sensitivity exceeds the required sensitivity gives a high degree of confidence that the required sensitivity can be achieved by a working instrument.

10. Adapting this spectrometer design to the Bendix MSDS 24 channel optical head is not feasible (Section 2.3.8).

The complete system as designed under this contract would have the following specifications:

Number of Spectral Bands	6
Wavelength & NETD (@ 25°C)	8.2 - 8.6 μm ≤ 0.3°C 8.6 - 9.0 μm ≤ 0.3°C 9.0 - 9.4 μm ≤ 0.3°C 9.4 - 10.2 μm ≤ 0.3°C 10.2 - 11.2 μm ≤ 0.3°C 11.2 - 12.2 μm ≤ 0.3°C
Primary Collecting Aperture Diameter	7.5 in.
Effective Optical Aperture	36 in.^{2}
Focal Length	13 in.
Scan Rate *(selectable)*	7.3; 8.7; 12 and 25 scans/sec.
V/H	.018; .021; .030; .062
Digitized Field of View	≥ 60°
Unvignetted Field of View	≥ 80°
Instantaneous Field of View	2.5 mrad
Roll Correction	±15°
Reference Sources	2 controlled thermal blackbodies
Digitization of Video	750 words/frame; 8 bit binary
HDDT Packing Density	10,000 BPI (Bi-ϕ-L coding)
Required Power	28 VDC; 2600 VA

Environmental:	*Temperature*	*Altitude*
Scan Head	-55°C to +50°C	0-46,000 ft.
Electronic Consoles	-10°C to +50°C	0-15,000 ft.

4
RECOMMENDATIONS

Since the conclusions based on the data presented in the report show that the AADS1285 will meet all of the objectives of the TIMS system as defined by JPL and NASA/NSTL, it is recommended that this sytem be fabricated and delivered to NASA as proposed by Daedalus under Contract NAS13-170.

The delivery of the AADS1285 system will give NASA and JPL an operational multispectral data collection capability that will be limited to the six thermal infrared bands specified. However, the design of the ABDE190 spectrometer allows this prealigned optical assembly to be removed from the scan head containing the primary optics and replaced without the need for realignment. This modularity indicates that it is feasible to design and build a series of interchangeable spectrometers for this scanner system. One such spectrometer could include the 1-2.5 μm bands which JPL has expressed an interest. Consideration should be given to funding additional effort to evaluate these options.

5
DESIGN PARAMETERS

5.1. OPTICAL COMPONENTS SPECIFICATIONS

Collimator Specifications

Type	Off-axis paraboloidal mirror
Effective Focal Length (EFL)	6.40" ± 0.02"
Optical Surface Accuracy	96% of the energy from a collimated source that fills the clear aperture into a circle of confusion no larger than 0.0005" at the focal plane
Substrate	Zerodur® manufactured by Schott Optical Glass
	Back surface flat is reference surface and must be perpendicular to OA within 0°1' [refer to Drawing #190B016]
Clear Aperture	4.050" minimum
Coating	Clear aperture shall be aluminized and overcoated with protective substance. Reflectance shall be 95% or greater between the wavelengths of 8.0 & 12.5 μm
Testing	EFL must be measured to within 0.001"
	Radius of radial V-groove must be measured to within ±0.001"
	Distance from back reference plane to focal point must be measured to within 0.001"
	Results of these measurements to be supplied with part

Diffraction Grating Specifications

Substrate Size	4.500" x 4.500" x 0.235"
Substrate Material	Zerodur®
Ruling	12 grooves per millimeter; parallel to edge of substrate ±0.5°
Incident Angle	25° from normal
Blaze Angle	3.37° ± 0.10°
Blaze Wavelength	9.1 μm
Efficiency	$\geq$ 90% at 9.1 μm
Wavelengths of Operation	8.2 to 12.2 μm

Imaging Lens Specifications

Lens Type	Germanium triplet - modification of Research Optical Systems Group P/N RGG-003V
Focal Length	75 mm ± 1 mm
f/N	0.62
A/R Coating	Each element surface shall be coated with HEA® coating process by Optical Coating Laboratories, Inc. to maximize transmission throughout the 8.2 to 12.2 m wavelength region. Alternate, equivalent coatings may be used with permission.
Lens Housing	Refer to Drawing #190D025
Back Focal Length (BFL)	0.75" ± 0.005° from reference surface A on Drawing #190D025
Temperature Compensation	BFL shall change by less than 0.0005" from its nominal value across a temperature range of -55°C to +50°C
Field of View	±1.5°
Resolution* On-Axis	40 μm
Resolution* Off-Axis	60 μm

*84% of the energy from a collimated source shall fall within a circle of the specified diameter at the focal plane.

Detector Array/Dewar Assembly Specifications

Detector Type	Photoconductive Mercury-Cadmium-Telluride (MCT)
Temperature	-55°C to +50°C
Altitude	0 to 50,000 ft.
Element Sizes	Refer to Drawing #190B001-A
Detectivities	cm-Hz$^{\frac{1}{2}}$-W^{-1} 10^{10} minimums as follows:

Element #	1	2	3	4	5	6
Bands λ μm	8.2-8.6	8.6-9.0	9.0-9.4	9.4-10.2	10.2-11.2	11.2-12.2
D*/10^{10}	2.7	2.8	2.9	1.8	1.9	1.8

Detector/System Electrical Bandwidth	DC to 50 KHz (-3 db)
Detector Field of View	With respect to normal at center of detector element. θ = ± 38.68° ± 1/2° (to accept beam from lens with f/N = .8). The entire array shall be restricted to this field of view by a cold shield where possible

Optical Filter	A LN_2 cooled bandpass optical filter shall cover the entire field of view of the array. The filter shall have a cut-on wavelength of 7.8 μm and a cut-off wavelength of 12.6 μm (5% transmission points). The performance of the filter shall equal or exceed the following: Transmission $\geq$ 70% absolute 8.2-12.2 μm Transmission $\geq$ 80% average 8.2-12.2 μm Transmission $\leq$ .1% absolute 4.0- 7.0 μm Transmission $\leq$ 1% absolute 2.0- 4.0 μm Transmission $\leq$ .1% absolute 13.0-16 μm The above specifications apply at 77°K in a vacuum environment. Spectral conformance will be based on a witness piece. Daedalus will supply the filters if vendor so desires. In that case, vendor to supply filter dimensions to Daedalus within 1 month ARO. Daedalus to supply filters 7 months ARO.
Dewar	Pour fill LN_2 dewar with holding time > 6 hours. (Suggest Cryogenics Associates metal dewar IR-13X or equivalent with a 5 psi pressure relief cap on the dewar chamber.)
Dewar Window	Germanium, with Optical Coating Labs., Inc. HEA® anti-reflection coating or equivalent for high transmission between 8 and 13 μm.
Mechanical	The center of the array shall be in the center of the dewar reference surface within 0.015".
Rotational Orientation	Array shall have a fixed orientation in the dewar with respect to either an identification mark on the dewar or with respect to a fixed feature of the dewar such as the connector pattern. If the fill port is off center, then element #1 must be aligned with the fill port center line with ±10° tolerance.
LN_2 Sensor	Sensor for low LN_2 signal (suggest silicon diode).
Connectors	Omni Spectra #OSM-242-8227 connectors provided for all electrical/electronic connections.

Dewar Data	Supply data on thermal coefficient of movement between dewar mounting surface and the detector array 4 weeks ARO.
Testing	Tests performed and data furnished for D* vs bias, relative spectral response, and responsivity vs bias for each element.

5.2. LIST OF PARTS DRAWINGS

ABDE117 Scan Head (TIMS)

MP11701 Hot Blackbody Outer Plate, Drawing #117C001
MP11702 Cool Blackbody Heat Sink, Drawing #117C002
MP11703 Reference Surface Plate, Drawing #117C003
MP11704 Cold Blackbody Top Plate, Drawing #117C004
MP11705 Cold Blackbody Insulator, Drawing #117B005
MP11706 Cold Blackbody Mounting Bar, .600 thick, Drawing #117B006
MP11707 Cold Blackbody Mounting Bar, .800 thick, Drawing #117B007
MP11708 Hot Blackbody Insulators, Drawing #117B008
MP11709 Secondary Mirror Mount, Drawing #117D009
MP11710 Thermal Compensation Sled, Drawing #117D010
MP11711 Scanner Support Beam, Drawing #117D011

ABDE190 Spectrometer (TIMS)

MTT1MS1 TIMS Detector Array, Drawing #190B001A
MP19001 Grating Holder Cover, Drawing #190B002
MP19002 Collimator Thermal Comp. Bar, Drawing #190B003
MP19004 Paraboloid Thermal Slide, Drawing #190B005
MP19005 Off-Axis Paraboloid Mount, Drawing #190B006
MP19006 Paraboloid Clamp, Drawing #190B007
MP19007 Paraboloid Base Clamp, Drawing #190B008
MP19008 Field Stop Adjustment Ring, Drawing #190B009
MP19009 Field Stop Cover with Seal, Drawing #190B010
MP19010 Field Stop Holder, Drawing #190B011
MP19011 Field Stop Retainer, Drawing #190B012
MP19012 Retainer Springs, Drawing #190B013
MP19033 Retainer Springs, Drawing #190B013
MP19013 Grating Holder, Drawing #190D014
MP19014 Collimator Base, Drawing #190D015
MP19015 Off-Axis Paraboloid, Drawing #190B016
MP19016 Field Stop, Drawing #190D017
MP19017 Diffraction Grating, Drawing #190D018
AC19001 Housing Assembly Details, Drawing #190D019
MP19003 Roll/Pitch Plate, Drawing #190D020
MP19018 X-Axis Adjustment Plate, Drawing #190D021
MP19019 Y-Axis Adjustment Plate, Drawing #190D022
MP19021 Dewar Mounting Plate, Drawing #190D024
MP19022 Lens Assembly Outline, Drawing #190D025
MP19023 Collimator Access Cover, Drawing #190D026
MP19024 Collimator Base Plate, Drawing #190D027

MP19025 Housing Plate, Drawing #190D028
MP19026 Housing Plate, Drawing #190D028
MP19027 Housing Plate, Drawing #190D028
MP19028 Housing Plate, Drawing #190D028
MP19029 Housing Plate, Drawing #190D028
MP19030 Housing Plate, Drawing #190D028
MP19031 P-R-Z Adjustment Post, Drawing #190D029
MP19032 P-R-Z Adjustment Wheel, Drawing #190B030
MP19033 P-R-Z Adjustment Spring Washer, Drawing #190B031
ABDE190 TIMS Assembly, Drawing #190D032
MP19034 Dewar Mount Assembly Cover Base, Drawing #190D033
MP19035 Dewar Mount Assembly Cover, Drawing #190D034

6
NEW TECHNOLOGY

The contract has not identified any reportable items relating to "new technology" as defined under Article GP-32 of Contract #955829.